

Comprehensive Catalogue of the Overall Best Distances and Properties of 402 Galactic Novae

Bradley E. Schaefer¹★,

¹*Department of Physics and Astronomy, Louisiana State University, Baton Rouge, Louisiana, 70820, USA*

10 October 2022

ABSTRACT

I derive the overall best distances for all 402 known galactic novae, and I collect their many properties. The centrepiece is the 74 novae with accurate parallaxes from the new *Gaia* data release. For the needed priors, I have collected 171 distances based on old methods (including expansion parallaxes and extinction distances). Further, I have collected the V-magnitudes at peak and the extinction measures, so as to produce absolute magnitudes at peak and then derive a crude distance as a prior. Further, I have recognized that 41 per cent of the known novae are concentrated in the bulge, with 68 per cent of these $<5.4^\circ$ from the galactic centre, so the 165 bulge novae must have distances of 8000 ± 750 parsecs. Putting this all together, I have derived distances to all 402 novae, of which 220 have distances to an accuracy of better than 30 per cent. I find that the disc novae have an exponential scale height of 140 ± 10 pc. The average peak absolute V-magnitude is -7.45 , with an RMS scatter of 1.33 mag. These peak luminosities are significantly correlated with the decline rate (t_3 in days) as $M_{V,peak} = -7.6 + 1.5 \log(t_3/30)$. The huge scatter about this relation masks the correlation in many smaller datasets, and makes this relation useless for physical models. The bulge novae are indistinguishable from the disc novae in all properties, except that the novae with red giant companion stars have a strong preference for residing in the bulge population.

Key words: stars: variables – stars: novae, cataclysmic variables

1 INTRODUCTION

Since the earliest days, astrophysics has had the difficult primary task of measuring the distances to objects of all classes. For the classical novae¹, measuring accurate distances has also long been an enterprise of the highest importance. Starting around the 1920s, novae were being distinguished as a separate class, distinct from other transients, with the nova distances bound up in the debates over the separate existence of galaxies as well as the separate existence of supernovae. Starting soon after the 1901 eruption of GK Per, a small number of novae had measured distances from the expansion parallax method, wherein the expanding nova shell had some vague edge matched to some poorly-defined radial velocity from an eruption spectrum. For many decades, the distances to individual novae were few and unreliable, with the best being the relative distances for the novae seen in globular clusters, the Magellanic Clouds, and the

Andromeda Galaxy. Even by the time of Payne-Gaposchkin's great treatise in 1964, little else was known.

Starting around the 1980s, a wide variety of distances for individual novae were put forth, all with poor reliability. A common on-going analysis of new novae would use some measure of the interstellar extinction, somehow calibrated, to derive distances, but such measures were uniformly poor and the calibrations had huge uncertainties. And measures of the observed peak magnitudes (and related quantities) were used with a wide variety of poorly calibrated correlations to get distances, but even the calibration novae displayed huge scatter, so any pretense for accuracy was not justified (Schaefer 2018). The best of the measures were from expansion parallaxes, while an impressive paper by Downes & Duerbeck (2000) used the *Hubble Space Telescope* (*HST*) to image 30 novae, collect all prior shell size data, and came up with 29 expansion parallax distances. Around this time, attempts were made to use novae to independently derive the distances to nearby galaxies and the Hubble Constant (Jacoby et al. 1992).

Starting around a decade ago, newly measured nova distances were being published with substantially better reliability. For the extinction distances, Özdönmez et al. (2018) systematically collected nova extinction measures and made good averages, and then used infrared sky surveys showing the tip of the red giant branch stars to provide a good calibration of the extinction as a function of distance along sightlines close to each nova. Parallaxes have always been the best method to get reliable distances to stars, and nova parallaxes

★ E-mail: schaefer@lsu.edu

¹ The classical novae (CNe) are cataclysmic variables (CVs) in binaries with a relatively ordinary companion star spilling mass into an accretion disc around a white dwarf, which display runaway thermonuclear explosions on the surface of the white dwarf (Warner 2008). These nova eruptions have outburst amplitudes ≥ 8 mags, rise times of days to weeks, and durations of weeks to many months (Payne-Gaposchkin 1964). An important class of CNe is the recurrent novae (RNe), which are ordinary novae that happen to have recurrence time-scales faster than a century (Schaefer 2010).

started to be produced, first for 4 novae with the *HST* by Harrison et al. (2013), then 3 novae with the first data release of *Gaia* (Ramsay et al. 2017), then I used the *Gaia* Data Release number 2 (DR2) parallaxes to report 41 accurate nova distances (Schaefer 2018).

The natural follow-up to the DR2 list of nova distances is to use the *Gaia* third data release (DR3) to construct a set of improved nova distance for many more novae. This is a primary goal of this paper. The new *Gaia* data provides good-accuracy distances to 74 novae. In addition, DR3 provides low-accuracy distances (often really just lower limits) for 121 novae. To realize these distances, the correct Bayesian calculations require the use of prior information, with such never having been assembled previously for any set of novae. This prior information needs the assembly of all prior published distances from all the many old methods found throughout the literature. Further, the prior information needs the magnitudes and extinctions for the many *Gaia* novae. So the correct use of the good and the poor *Gaia* parallaxes requires a large scale data mining program.

Once we have the idea of making a large catalog of the best distances for the *Gaia* novae, a natural extension is to get the best distances for *all* known galactic novae. For the novae not in *Gaia* DR3, all we have is a collection of non-parallax data. For roughly a third of the novae, the only useful information is the galactic position. For the bulge novae, this turns out to give accurate and reliable distances. For the disc novae, the position alone can provide distance constraints with the uncertainty of order $3\times$ from the central estimate, and that is adequate for many purposes. So my program is extended to provide the best possible distances for all galactic novae.

The first step of the program is to construct a complete census of known galactic novae for peaks with all times before middle 2022. This list was constructed from partial lists in Duerbeck (1987), the Catalog and Atlas of Cataclysmic Variables (CVCat, Downes et al. 2001, updated to 2005), the International Variable Star Index² (VSX) of the American Association of Variable Star Observers, and the up-to-date list³ of K. Mukai (NASA HEASARC). In most cases, the status as a nova is clear from the light curve and spectra, however, roughly a dozen systems are poorly observed so that the nova status is questionable, and for this I have followed the always excellent judgement of H. Duerbeck in his very useful catalog (Duerbeck 1987). For inclusion in my list, I required good evidence that the transient was indeed a classical nova. My list does not include the red novae (like V838 Mon and V1309 Sco), the symbiotic novae (like PU Vul and V1016 Cyg), the X-ray novae (like V404 Cyg and V616 Mon), nor systems that show only dwarf nova events (like WX Cet and WZ Sge), because these eruptions are all morphologically greatly different, the systems have different evolution, and are dominated by different mechanisms. In the end, I have 402 systems that are confidently galactic novae.

2 NOVA DISTANCES FROM ALL THE OLD METHODS

The olden standard for nova distances has been the expansion parallax. Schaefer (2018) used *Gaia* DR2 parallaxes and found that the real accuracy has a one-sigma error bar of 0.95 mag in the distance modulus. Here, I have collected 38 expansion parallax distances as previously collected in Schaefer (2018) and Özdönmez et al. (2018).

A traditional astronomy method for getting nova distances is to somehow measure the extinction from the intervening interstellar

medium (ISM), then to calibrate the extinction as a function of distance along the line of sight to the nova. The olden extinction distances were always poor. A useful new tool has been the reddening maps showing $E(B - V)$ for the entire line of sight through our galaxy, all with high accuracy for lines-of-sight within 5 arc-minutes of any target, as based on the far-infrared dust emission (Schlafly & Finkbeiner 2011). Recently, a good advance has been made by Özdönmez et al. (2018), where the extinction as a function of distance is calibrated from the brightness and color of red clump stars observed by several deep infrared sky surveys. Özdönmez et al. reports on 81 reddening distances, including 29 lower limits on distances. Schaefer (2018) found that these reddening-distances have a one-sigma uncertainty of 1.01 mag in the distance moduli.

Here, I introduce another method based on extinction. The idea is that the total extinction throughout the Milky Way along every line of sight is known from infrared mapping (Schlafly & Finkbeiner 2011), so for systems with substantially less than the maximum, we can quantitatively estimate the nova distance. For example, V4742 Sgr has the maximum possible extinction of 5.65 mag, while its measured $E(B - V)$ is 1.5 ± 0.2 . With the majority of the line-of-sight extinction occurring within the region around the centre of our galaxy, V4742 Sgr must be substantially closer than 8000 pc. To be quantitative, I have modeled the Milky Way dust as the usual axisymmetric exponential disc, with a scale height of 100 pc out of the galactic plane, and with a scale length of 3200 pc in its galactocentric radius distribution (Li et al. 2018). From an integral within this model, I calculate the dust column density as a function of distance from Earth, and scale this by the maximum $E(B - V)$ for the entire column through our Milky Way. The observed extinction can then be matched to distance, and this can be converted to a distance modulus. For V4742 Sgr, the observed extinction corresponds to a distance of 3120 ± 380 pc, or a distance modulus of $\mu=12.47\pm 0.26$. The formal error bars are likely much too small, partly because the real dust in our galaxy is much more clumpy than in the standard model. I will adopt the same one-sigma uncertainty of 1.01 mag, as in the previous paragraph. The results from this method are superseded by the better calibration of Özdönmez et al. (2018). The only novae for which this method provides useful constraints are KY Sgr, V4742 Sgr, V4744 Sgr, V5586 Sgr, and V1662 Sco.

A physics method for nova distances is to get a blackbody distance to the companion stars. I have collected 7 blackbody distances from Schaefer (2010), Salazar et al. (2017), and Shara et al. (2017a).

Another physics method is to model the eruption light curve of an individual nova, scale the time to a universal law, so as to derive the peak absolute magnitude, which then gives the distance modulus. I. Hachisu (University of Tokyo) and M. Kato (Keio University) are the only modelers with this method, from which I have collected 68 nova distances as reported in Hachisu & Kato (2021) and references therein. Schaefer (2018) found that these measures have a one-sigma uncertainty of 0.76 mag in the distance moduli.

The *HST* has been able to measure good parallaxes for four of the nearest and brightest novae; V603 Aql, DQ Her, GK Per, and RR Pic (Harrison et al. 2013). Schaefer (2018) found these four measures to be substantially poorer than the quoted error bars, with the average one-sigma uncertainty being 0.37 mag in the distance moduli.

A unique method for measuring a nova distance has been presented by Sokolowski et al. (2013) for the RN T Pyx, wherein the light echo as reflected by the previously ejected nova shells is used similarly to the expansion parallax.

Two novae are known to appear inside galactic globular clusters, with the nova positions being sufficiently close to the cores so that the membership in the cluster is not in any doubt. The old nova T

² <https://www.aavso.org/vsx/>

³ <https://asd.gsfc.nasa.gov/Koji.Mukai/novae/novae.html>

Table 1. Compilation of Nova Distances from Old Methods (full table with 171 novae is in on-line supplementary material)

Nova	D (pc)	μ_{old} (mag)	Method
OS And	7300	14.32 ± 0.76	Model
CI Aql	3900	12.96 ± 1.01	Extinction
V500 Aql	5900	13.85 ± 0.95	Expansion
V603 Aql	249	6.98 ± 0.37	<i>HST</i> ϖ
V1229 Aql	2400	11.90 ± 0.95	Expansion
...			
PW Vul	1800	11.28 ± 0.95	Expansion
QU Vul	3140	12.48 ± 0.95	Expansion
QV Vul	2700	12.16 ± 0.95	Expansion
V458 Vul	> 6000	$> 13.89 \pm 1.01$	Extinction
V459 Vul	3800	12.90 ± 0.76	Model

Sco is in the globular M80, while Nova 1938 Oph is in M14. The distances to the host globular clusters are taken from the *Gaia* EDR3 parallaxes for over 600 member stars (Vasiliev & Baumgardt 2021).

These distances are collected into Table 1. The first column gives the nova designation, with the novae listed in the standard order as in the General Catalog of Variable Stars (GCVS). The second column gives the reported old distances, in parsecs. The third column gives the associated distance modulus and its assigned one-sigma uncertainty. The last column gives the method for the old distance, with 38 expansion parallaxes, 87 distances and limits based on extinction, 7 blackbody distances from the companions, 32 distances based on the physics models of Hachisu & Kato, 4 parallax distances from *HST*, 1 light echo distance for T Pyx, and 2 distances for the host globular clusters. For all of the old methods, I have a total of 171 distances, of which 29 are lower limits on the distance.

3 DISTANCES BASED ON THE PEAK MAGNITUDES

Despite the historical confusions, there is good information on nova distances from the peak magnitudes, and this method can be applied to most old novae. Indeed, for many novae, the peak magnitude provides the only specific information on D . Even for those novae with *Gaia* parallaxes, the distances from the peak magnitudes will form the primary basis for the priors as used in the Bayesian calculation of the parallax-distances.

For my plan of getting the best distance information for all 402 galactic novae, I need to collect the peak magnitudes and extinctions for all the novae that were observed at maximum. More specifically, I need the observed peak V -band magnitude, V_{peak} , as well as the color excess, $E(B - V)$. These will be used to calculate the distance modulus, μ_{peak} .

In bureaucratic mode, we could just look up the peak magnitudes in various catalogs, but such would be poor for the majority of the novae. A primary problem is that the usual tabulations often are listing only the maximum observed brightness, which might or might not be at the real peak, or worse will list some speculative peak magnitude based on extrapolation. Another big problem is that the peak magnitudes are often in a wide variety of band passes other than V -band, with the applicable band being often unstated, whereas some correction is needed to get to V_{peak} . These problems can be confidently solved for over a hundred of the brightest novae, with these being well observed and reported in the literature. The best source is Strope, Schaefer, & Henden (2010) for the 93 all-time (before 2010) best observed novae, because this work went back and pulled out all the light curves, from all the published literature, from the entire AAVSO database, plus

extensive measures of my own from the Harvard plates. Another reliable source is Duerbeck's catalog (Duerbeck 1987) for all novae up until 1987, as he also went back to the entire literature plus going back to the original photographic plates of old, and his evaluations are excellent. Another reliable source is C. Payne-Gaposchkin's great treatise (Payne-Gaposchkin 1964), also with references to the full literature and a deep knowledge of the Harvard plates. Even with these excellent compilations, the majority of the novae still have either unlisted or questionable peak magnitudes. At this time, the only way to produce reliable measures of V_{peak} or its limit is to go through the entire literature and AAVSO database exhaustively for roughly 300 novae.

To get a useable distance modulus, we also need a reliable measure of extinction. For this, the literature contains useful measures of $E(B - V)$, or its equivalent, for only the brighter novae, and these are often contradictory and always scattered by much more than the quoted error bars. Özdönmez et al. (2018) compiled an exhaustive and excellent summary of the scattered literature to make judicious evaluations for the $E(B - V)$ of 178 galactic novae. This provides the foundation for my tabulation of $E(B - V)$. But we still need some sort of an estimate for the remaining 224 galactic novae. For this, a wonderful tool is the all-sky catalog of $E(B - V)$ through the entire line of sight through our Milky Way galaxy (Schlafly & Finkbeiner 2011). This serves to put an approximate-but-strict upper limit on $E(B - V)$. For some novae, this upper limit serves as an adequate constraint, while many other of the faintest novae away from the galactic plane must have their extinction close to the limit (as the nova is certainly far past all galactic dust). For the roughly 200 novae without useful limits from Özdönmez or Schlafly & Finkbeiner, the only solution is to go through the literature and data for effective evidence on the extinction. I have also pulled out good measures of extinction by extracting the V_{peak} and B_{peak} from the magnitudes scattered through the literature (see below).

While doing these exhausting and exhaustive searches of the literature and databases, I have also tabulated the best information on a variety of other nova properties. From my new light curve compilations, I have classified 265 light curves into the classes S, P, O, C, D, J, and F (Strope et al. 2010). These light curve classes are strongly correlated with a variety of nova properties. From the literature (primarily the Strope catalog and the Duerbeck catalog) and from my own compilations of the light curves, I have measured both t_2 and t_3 (the number of days for the nova light curve to decline from peak magnitude by 2 and by 3 magnitudes). From all this, I have only been able to extract 262 and 252 reliable measures of t_2 and t_3 respectively. I have also compiled lists of the spectral classifications for 259 nova, with the classes being Fe II, He/N, and Hybrid, as well as whether it is a Neon Novae. I have also compiled a list of the shell expansion velocity for 216 galactic novae, as measured by the FWHM of the $H\alpha$ line. This measure changes substantially with the development over time, and the literature often only reports the FWHM of other hydrogen lines or the FWZI of the Balmer lines, so this compilation has inhomogeneities at perhaps the 30 per cent level. My list of spectral classes and FWHM values is just a large extension of the list presented in Pagnotta & Schaefer (2014). Schaefer (2022) has already compiled a list of the orbital periods for 156 galactic novae, with this list including 49 newly discovered orbital periods and the list is $2\times$ longer than previous lists. Finally, I have also compiled the galactic coordinates for all 402 novae, mainly from the VSX database.

Importantly, I have been careful for distinguishing whether the true peak was observed. For inclusion in my list of measured V_{peak} , I require some suitable evidence that the brightest observed magnitude

is close in time to the real peak. This evidence is usually an observed rise to maximum, or a useful closely-spaced pre-eruption limit, or a spectroscopic ‘age’. When multiple measures on the night of peak are available, I use the nightly average. When I determine that the nova light curve does not reliably represent the true maximum, I list the V_{peak} as a limit.

The light curves and the tabulated peak magnitudes are usually in the V -band, however, 102 nova from before 1973 have only B -band light curves, almost always based on the archival Harvard plates. The spectral sensitivity of these plates is essentially identical to that of the Johnson B -band, so there is no color-term for the reported magnitudes. The peak magnitudes for novae are always in the bright regime, where the comparison stars are accurately on the modern magnitude scale. So the magnitudes reported for the Harvard plates (and the Sonneberg plates) are all reliably in the modern B -band. For these novae, we must convert from B_{peak} to V_{peak} as

$$V_{peak} = B_{peak} - E(B - V) - \langle (B - V)_{peak,0} \rangle. \quad (1)$$

The last term is the intrinsic color at peak. This color is nearly a constant from nova-to-nova, having to do with the temperature of the photosphere in the expanding nova shell being determined by the ionization temperature of hydrogen.

This intrinsic color at maximum has long been realized to be approximately 0.0 mag. The only systematic measure that I know of is from van den Bergh & Younger (1987), who used 7 novae (after discarding two outliers) to get +0.23 mag, with an RMS scatter of 0.16 mag. I can improve substantially on this old value by using 24 nova with the uncertainty in the extinction of 0.10 mag or less, as listed in GCVS order in Table 2. The second column gives the light curve class (‘LC’), with the point to be that the intrinsic color at maximum light does not depend significantly on the class of the nova. The next two columns give my measure of the observed $B - V$ at the time of peak light in the V -band and my estimated $E(B - V)$ as based on methods not involving the nova colors, both in units of magnitudes. The last column gives the derived $(B - V)_{peak,0}$. The RMS scatter of the intrinsic colors (0.19 mag) effectively equals the average uncertainty for all 24 novae (0.18 mag), which means that the observed scatter is all measurement errors and the underlying distribution is consistent with being a single constant. The average intrinsic color is $\langle (B - V)_{peak,0} \rangle = +0.11 \pm 0.04$ mag.

For novae that have well measured peaks in both the B and V , equation (1) can be turned around to get a good measure of the $E(B - V)$. This is useful for the many faint novae that are too faint to have had any useful measure of the extinction from spectroscopy.

My collected V_{peak} and $E(B - V)$ values for all 402 galactic novae are presented in Table 3. The first column is the nova in GCVS order. The next two columns give the best V_{peak} and $E(B - V)$ values.

To get the distance modulus, we also have to have an independent measure of the absolute magnitude at peak, $M_{V,peak}$. Schaefer (2018) has already demonstrated that the various historical calibrations are poor. So I do not know of any means to produce the best peak absolute magnitude that is any better than just taking the average. Schaefer (2018) used *Gaia* DR2 parallaxes to find the average $M_{V,peak}$ is -7.0 mag, with a one-sigma scatter of 1.4 mag.

My values of V_{peak} and $E(B - V)$ are combined with the adopted $M_{V,peak}$ to produce a distance modulus, μ_{peak} . To be specific,

$$\mu_{peak} = V_{peak} - 3.1E(B - V) - (-7.0). \quad (2)$$

The uncertainties are calculated from the usual propagation of errors for each of the terms. My derived μ_{peak} values are tabulated in the fourth column of Table 3 for all 402 galactic novae.

The uncertainty on the distance modulus is always ± 1.4 mag or

Table 2. Intrinsic Color at Peak, $(B - V)_{peak,0}$

Nova	LC	$(B - V)_{peak}$	$E(B - V)$	$(B - V)_{peak,0}$
OS And	D	0.44 ± 0.14	0.15 ± 0.05	0.29 ± 0.15
V705 Cas	D	0.60 ± 0.14	0.41 ± 0.06	0.19 ± 0.15
V1065 Cen	P	0.49 ± 0.28	0.47 ± 0.05	0.02 ± 0.28
FM Cir	J	0.30 ± 0.28	0.23 ± 0.05	0.07 ± 0.28
V394 CrA	P	-0.20 ± 0.14	0.20 ± 0.10	-0.40 ± 0.17
T CrB	S	0.50 ± 0.14	0.10 ± 0.10	0.40 ± 0.17
V1500 Cyg	S	0.64 ± 0.14	0.45 ± 0.07	0.19 ± 0.16
V1668 Cyg	S	0.68 ± 0.14	0.38 ± 0.05	0.30 ± 0.15
V1974 Cyg	P	0.50 ± 0.14	0.26 ± 0.03	0.24 ± 0.14
V2491 Cyg	C	0.41 ± 0.14	0.23 ± 0.05	0.18 ± 0.15
V339 Del	PP	0.25 ± 0.14	0.18 ± 0.04	0.07 ± 0.15
V408 Lup	J	0.68 ± 0.14	0.40 ± 0.10	0.28 ± 0.17
T Pyx	P	0.30 ± 0.14	0.25 ± 0.02	0.05 ± 0.14
V4739 Sgr	S	0.55 ± 0.14	0.46 ± 0.04	0.09 ± 0.15
V5579 Sgr	D	0.73 ± 0.14	0.72 ± 0.06	0.01 ± 0.15
V5583 Sgr	S	0.42 ± 0.28	0.34 ± 0.10	0.08 ± 0.30
V5668 Sgr	D	0.40 ± 0.14	0.21 ± 0.10	0.19 ± 0.17
V6594 Sgr	P	0.36 ± 0.14	0.30 ± 0.05	0.06 ± 0.15
U Sco	PP	0.30 ± 0.14	0.20 ± 0.10	0.10 ± 0.17
NR TrA	J	-0.08 ± 0.28	0.22 ± 0.05	-0.30 ± 0.28
V382 Vel	S	0.06 ± 0.14	0.12 ± 0.03	-0.06 ± 0.14
LV Vul	S	0.95 ± 0.14	0.57 ± 0.05	0.38 ± 0.15
QV Vul	D	0.66 ± 0.14	0.40 ± 0.05	0.26 ± 0.15
V458 Vul	J	0.55 ± 0.28	0.50 ± 0.05	0.05 ± 0.28

Table 3. Distance Moduli from V_{peak} With $M_{V,peak} = -7.0 \pm 1.4$ (full table with 402 novae is in on-line supplementary material)

Nova	V_{peak} (mag)	$E(B - V)$ (mag)	μ_{peak} (mag)
OS And	6.50 ± 0.10	0.15 ± 0.05	13.04 ± 1.41
CI Aql	9.00 ± 0.10	0.85 ± 0.30	13.37 ± 1.68
DO Aql	8.50 ± 0.10	0.29 ± 0.10	14.60 ± 1.44
EL Aql	5.32 ± 0.18	0.97 ± 0.15	9.31 ± 1.49
EY Aql	9.69 ± 0.54	1.10 ± 0.50	13.28 ± 2.16
...			
QV Vul	7.10 ± 0.10	0.40 ± 0.05	12.86 ± 1.41
V458 Vul	8.10 ± 0.20	0.50 ± 0.05	13.55 ± 1.42
V459 Vul	7.60 ± 0.10	0.86 ± 0.12	11.93 ± 1.45
V569 Vul	$<16.3 \pm 0.20$	3.06 ± 0.50	$<13.81 \pm 2.10$
V606 Vul	10.10 ± 0.10	0.86 ± 0.20	14.43 ± 1.53

somewhat larger, which is a reflection of the fact that we cannot independently know the real luminosity of the nova with any good accuracy. This relatively poor accuracy is still useful for some purposes, including distinguishing bulge from disc novae. For many novae, this will be the only useful specific information of their distances. These V_{peak} -distances will also provide the prior information used in the Bayesian calculations from the *Gaia* parallaxes. For the novae with accurate *Gaia* parallaxes, the V_{peak} -distances will have little effect on the final range of distances. For the majority of novae with relatively poor *Gaia* parallaxes, the V_{peak} -distances will provide a prior that will force the result towards the near or far side of the range allowed from the parallaxes.

4 DISTANCES TO BULGE NOVAE

The distribution of galactic novae across the sky (see Fig. 1) shows two distinct populations. The well-known novae (because they are

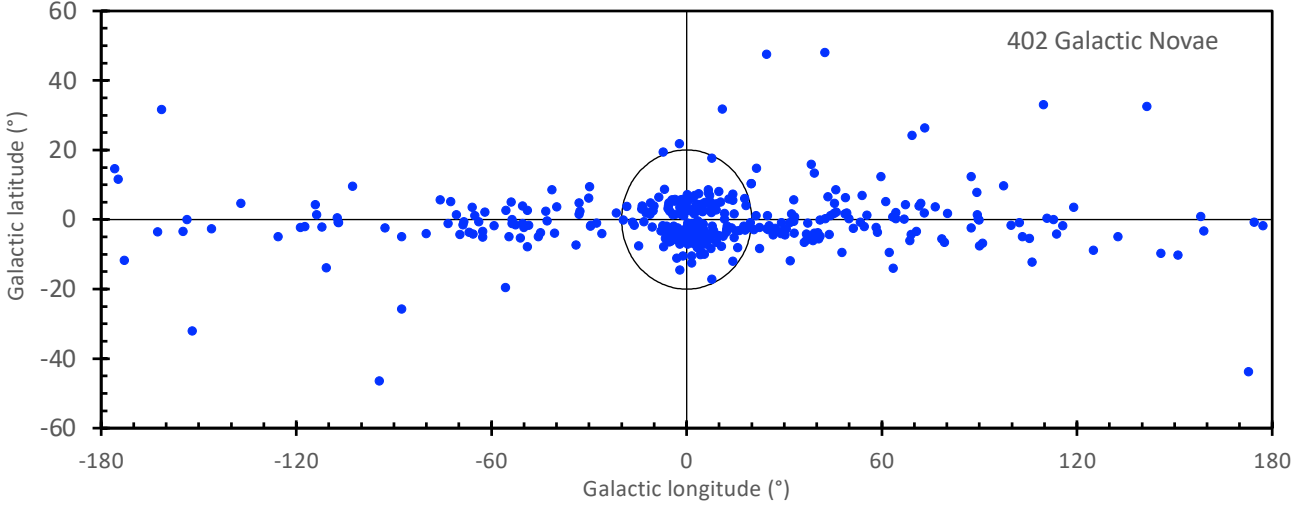


Figure 1. Galactic distribution for 402 novae. The nova distribution is the sum of a disc population (over all galactic longitudes and mostly within 10° of the galactic plane) and the bulge population (mostly within 9° of the galactic centre, and all within the 20° circle in the plot). Nearly 41 per cent of all discovered novae are in this small clump. With this positional information alone, we see that any nova within something like 9° of the galactic centre has a high probability of being a bulge nova. The gap at low galactic latitudes is prominent for the bulge novae, because they are roughly at 8000 pc distance and dimmed by very high extinction. The low-latitude zone-of-avoidance is not significantly visible outside of the bulge.

Table 4. Bulge/Disc Population Identification for $\theta_{GC} < 20^\circ$ (full table with 214 novae is in on-line supplementary material)

Nova	θ_{GC} ($^\circ$)	μ_{old} (mag)	μ_{peak} (mag)	ϖ (mas)	Population
V5854 Sgr	1.00	...	$< 11.90 \pm 3.13$	1.43 ± 1.41	bulge
V3730 Oph	1.57	...	$< 12.60 \pm 2.10$	-0.08 ± 0.70	BULGE
V4092 Sgr	1.77	...	$< 14.09 \pm 1.69$...	bulge
V2415 Sgr	1.77	...	$< 16.09 \pm 1.72$...	bulge
V5586 Sgr	1.79	12.74 ± 1.01	11.90 ± 1.69	...	DISC
...					
V1313 Sco	18.85	15.25 ± 0.76	13.71 ± 1.75	...	BULGE
V841 Oph	19.29	...	10.06 ± 1.49	1.19 ± 0.02	DISC
V366 Sct	19.53	...	$< 5.90 \pm 9.87$	-0.32 ± 1.53	DISC
V1662 Sco	19.59	12.29 ± 1.01	$< 11.30 \pm 4.86$...	DISC
FV Sct	19.68	...	$< 14.13 \pm 1.92$	0.48 ± 0.22	disc

bright from being close our Sun) are in the disc population, which appear close to the galactic plane all around the galactic equator. The bulge novae (those that cluster within 20° of the galactic centre) are clearly a distinct population. This division of novae into disc and bulge populations is similar to the division of all Milky Way stars into disc and bulge populations. Presumably the bulge novae are just an ordinary part of our galaxy’s bulge, and represent an older population. All of the bulge novae are relatively faint (none peaking brighter than 7.3 mag), and so there are no famous bulge novae.

With the bulge novae being faint and obscure, little work has been done on their distinct properties. Shafter (2008) provides a review of the results. Estimated bulge fractions ranges from some small percentage (Duerbeck 1984) up to around 75 per cent (Della Valle & Livio 1994). With a detailed model of structures for the bulge stars, disc stars, and interstellar extinction, Hatano et al. (1997), concluded “the true bulge fraction of Galactic classical novae is much closer to $1/8$ than to $1/2$, i.e., most Galactic classical novae are from the disc, not from the bulge”. With these large uncertainties, Shafter points out that external galaxies became the focal point for population studies. Unfortunately, this produced contradictory studies on key properties, for example, whether of not the $M_{V,peak}$ is bimodally distributed or

not, and on whether the specific rates (novae per year per unit stellar mass) are correlated with the Hubble type of the galaxy. And we recently have the conundrum that our Milky Way has 15-out-of-20 novae with evolved companions in the bulge population (Schaefer 2022), while the Andromeda Galaxy apparently has all of such nova in the disc population (Williams et al. 2016). It is safe to say that little is known with useable confidence about the galactic bulge nova demographics and properties. For example, I know of no listing of galactic bulge novae, much less a compilation of their properties.

The defining property of the bulge novae is their angular distance from the galactic centre, θ_{GC} . For this, I have calculated θ_{GC} for all 402 nova, and constructed a histogram for the density of novae inside annuli of 1° widths, in units of number-per-square-degree (Fig. 2). This histogram shows two distinct populations, the high clump with $\theta_{GC} < 20^\circ$ for the bulge novae plus the low-flat component over all θ_{GC} for the disc novae.

What is the disc component for $\theta_{GC} < 20^\circ$? It is possible to try to use a detailed galactic model, but such would not have much confidence due to not knowing how nova systems relate to the other stars in the general model. For any model or empirical results, high accuracy will not be possible, because we are dealing with small-

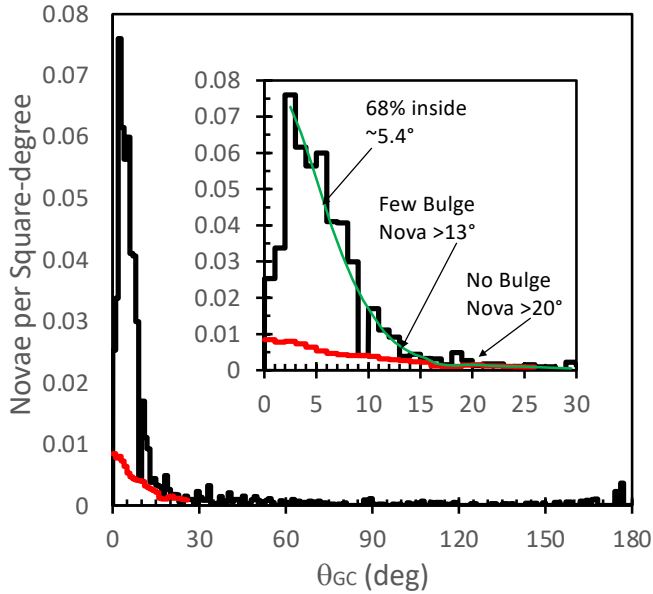


Figure 2. Distribution over angle from galactic centre for 402 novae. One important point from this figure is to see the huge and narrow cluster of novae closely around the galactic centre, with these being the bulge population. This cluster is shown with an expanded angular scale in the inset figure. The best estimate for the number density of disc novae for the galactic centre region is shown by the red histogram. In the densest part of the bulge area, the probability that a nova is in the bulge varies from roughly 80–90 per cent, as based on the θ_{GC} alone. We see that few bulge novae appear with $\theta_{GC} > 13^\circ$, and no bulge novae appear more than 20° from the galactic centre. A description of the bulge population distribution is that of a Gaussian with a sharp drop in the innermost region due to interstellar dust. While the small-number statistics and the dust absorption make for substantial uncertainties, the 68 per cent containment radius is roughly 5.4° . For a distance to the galactic centre of $D_{GC} = 8000$ pc, this corresponds to a characteristic radius for the bulge population of $R_{bulge} = 750$ pc.

number statistics, with there being 3 or fewer disc novae in each annulus. There are also large systematic errors in the nova detection rates around the galactic centre, as can be seen by the large differences between negative and positive longitudes, as well as by the asymmetries between the positive and negative latitudes near the centre. These asymmetries are likely caused by a combination of the complex history of nova search regions as well as in the galactic dust absorption. With these asymmetries, there is no accurate means to interpolate the disc population into the galactic centre region. A reasonable empirical method is to make identical counts in annuli for cases where all the nova coordinates are shifted by a constant in galactic longitude. So for example, if all the longitudes are shifted by $+40^\circ$, we have just 1 nova inside the 4.0° to 5.0° annulus, and if the longitudes are shifted by -40° then we have 2 novae. This is while the real sky, i.e., with zero shift, has 20 novae in the same annulus, so we can divide these up into approximately 18–19 bulge novae and 1–2 disc novae. This preserves the statistics of the galactic latitude distribution as combined with the annuli shape, and it ensures that we are only counting disc novae. To get useable statistics, I have evaluated the number in each of the shifted annuli for shifts of $\pm 50^\circ$, $\pm 40^\circ$, $\pm 30^\circ$, and $\pm 25^\circ$ for small annuli. There is no significant rise in numbers from 50° to 25° . Averaging over these shifts and then smoothing over angles produces my best estimate for the numbers

and densities of disc novae inside the galactic centre region. This is displayed as the red line in Fig. 2.

The bulge component rises high above the disc component for $\theta_{GC} < 9^\circ$. For these novae, by the galactic coordinates alone, the probability is high that any individual nova is in the bulge population. The huge excess of bulge novae in Fig. 2 falls off sharply from 5° to 13° . A case can be made that the observed number of novae outside 13° is nearly consistent with the expected numbers from the disc population. The excess in the observed novae over the expectations for disc novae alone is just 15 novae from $13^\circ < \theta_{GC} < 20^\circ$, and with the uncertainties, this is barely a ‘ $3\text{-}\sigma$ ’ result. The density for bulge novae outside of 20° is certainly negligible.

What is the characteristic radius of the bulge population, R_{bulge} ? I will describe this characteristic radius using terminology for a Gaussian distribution, with this usage as a reasonable description rather than a model or theory claim. The measure of the 68 per cent containment radius has substantial uncertainties due to the uncertain variation around any smooth curve (see inset in Fig. 2), the uncertainties in the numbers of disc novae to subtract out as ‘foreground’, and the sharp drop in numbers at the lowest galactic latitudes. Nevertheless, I have fitted a Gaussian for the annuli from $2\text{--}20^\circ$. The Gaussian sigma is 5.4° . The formal error bar is 0.3° . But I expect that the real error bar is larger due to systematic problems, most importantly due to the substantial changes in the nova discovery efficiency across the galactic centre region, and the real uncertainty is more like $\pm 1^\circ$.

The distance to the galactic centre, D_{GC} , has long been measured, and with increasing accuracy. Reid (1993) reviewed all the prior measures and concluded that $D_{GC} = 8000 \pm 500$ pc. Malkin (2012) reviewed 52 measures of the distance from 1992–2013, yielding a final combined best distance of $7980 \pm 15 \pm 20$ pc. To all needed accuracy, I will adopt the round-number of $D_{GC} = 8000$ pc.

Now, we can turn the characteristic angular size of the bulge nova population into its physical size. This is simply $R_{bulge} = D_{GC} \sin(5.4^\circ)$, or 750 pc, with an uncertainty of roughly ± 130 pc. With this, along any line of sight towards the galactic centre, every bulge nova must have a distance of 8000 ± 750 pc, with the uncertainty containing 68 per cent of the population. This distance corresponds to a distance modulus of 14.5 ± 0.2 mag and corresponds to a simple parallax of 0.125 ± 0.012 milli-arcseconds (mas).

Now, with my compilation of all 402 known novae, I can pick out a complete roster for the bulge population novae, with good confidence for each individual nova. The first cut, based on the drop to no-excess above the disc nova population, is that bulge novae are only with $\theta_{GC} < 20^\circ$. Next, I require that each candidate bulge nova have a *Gaia* parallax (if available) consistent with 0.125 mas. Most bulge novae are too faint to have a *Gaia* parallax, so this requirement is mainly used to identify disc novae in the galactic centre region as those with a parallax too large to be consistent with the bulge distance. Further, I require that μ_{peak} be consistent with 14.5 mag. Most bulge novae have poor measures of μ_{peak} , so this constraint is mainly useful for recognizing disc novae that are too bright to be bulge novae. Plus, I require that any available old distance measures from the literature be consistent with D_{GC} , which is to say that μ_{old} is consistent with 14.5 mag. For the 214 novae with $\theta_{GC} < 20^\circ$, I have placed the values of μ_{old} , μ_{peak} , and the *Gaia* parallaxes (see next Section) into Table 4. These can be used to find consistency or inconsistency for each nova with a distance of D_{GC} .

Further constraints on the nova distances can be derived from their observed extinctions and magnitudes: (1) If the observed extinction is greatly smaller than possible for a ~ 8000 pc distance, then the system must be a disc nova. For the best example, consider V4643 Sgr, with its position close to the galactic centre and b of -0.34° . The

total extinction along this heavily-shrouded line-of-sight is 20.5 mag (Schlafly & Finkbeiner 2011), so if V4643 Sgr were inside the bulge then its extinction would be >10 mag or so. However, the observed extinction is 1.47 ± 0.20 mag, and hence the nova must be much closer than the bulge and must be part of the disc population. For a different example, V366 Sct was observed to peak at 9.94 mag, but we have no measure of its extinction. The line-of-sight has 8.4 mag of extinction (Schlafly & Finkbeiner 2011), so a bulge nova must have $E(B - V) > 4$ mag or so, for $A_V > 12$ mag. To be in the bulge, V336 Sct would need a peak absolute magnitude more-luminous than -16 mag, which is certainly not a nova. This method can demonstrate that 10 novae in the galactic centre region are certainly of the disc population. **(2)** A further constraint comes from the quiescent magnitudes with extinction corrections, $V_{q,0}$. This uses my earlier result that novae in quiescence almost always have an absolute magnitude more-luminous than $+5$ mag (Schaefer 2018; see also Patterson et al. 2022). So any nova appearing with $V_{q,0} > 19.5$ is unlikely to be in the disc population. For the specific example of V4444 Sgr, the extinction is 0.56 mag or less (Schlafly & Finkbeiner 2011), the quiescent magnitude is >21 (CVCat), so the distance modulus must be >14.3 , which demonstrates a bulge population. Twelve novae in the galactic centre region are thus shown to be bulge novae. **(3)** A similar constraint comes because few classical novae have quiescent absolute magnitudes more-luminous than $+3$ mag. The only exceptions are RN and those systems with subgiant and giant companions, with these being recognized by their infrared colors, even at bulge distances (Schaefer 2022). Hence, a normal bulge nova (with a distance modulus near 14.5 mag) will appear fainter than 16.5 mag. This can be turned around to say that a nova with $V_{q,0} < 16.5$ is likely a disc nova. For example, V732 Sgr is seen at $V_q = 16.9$ (Mroz et al. 2015) with extinction of 0.81 ± 0.16 mag, so $V_{q,0} = 14.4$ at the distance of the bulge the absolute magnitude would have to be more-luminous than -0.1 mag, which is to imply that the system is in the disc population. With this method, five novae in the galactic centre region can be assigned to the disc population.

For many novae, the evidence is clear as to whether the nova is bulge or disc. These are indicated in the last column of Table 4 with either “DISC” or “BULGE”. Out of the 214 novae in Table 4, 124 have a confident population assignment. Most disc novae will have a clear signature. That is, they are usually bright enough to have one of the ‘old’ methods applied, or to have their $\mu_{peak} \ll 14.5$, or to be near enough that *Gaia* can detect a large parallax. I find 14 disc novae for $0^\circ < \theta_{GC} < 6^\circ$, 17 disc novae from 6° to 12° , and 4 disc novae in the range 12° – 18° , with this being consistent with my prior estimates.

Nevertheless, many novae in Table 4 do not have a confident population. A good case can be made that the remaining novae are almost all in the bulge population. First, such novae will be those that are relatively faint and relatively far, which is to say that most of the cases will be bulge novae. Second, roughly all of the disc novae in the bulge cluster of Fig. 2 are now identified, and the remaining novae can only be bulge sources so as to account for the huge excess at low θ_{GC} . For example, in the 0 – 6° zone, 9 disc novae are expected, 14 disc novae are now confidently identified, and the zone has 83 novae, so nearly all of the $83 - 14 = 69$ remaining novae must be bulge systems. Similarly, for the 6 – 12° zone, 17 disc novae are expected, 17 disc novae have been identified, so the remaining 75 novae must be almost entirely bulge novae. In the 12 – 18° zone, the 24 remaining novae (i.e., those not already identified as being disc population) must have 14 or more that are bulge systems.

I can present a good case for the probability being high for many of the novae being bulge systems, even without any good *Gaia* parallax or other data. In the 0 – 12° zone, the probability of such stars being

a bulge system is ≥ 95 per cent, simply as required to make the bulge contribution in Fig. 2 while all the disc novae are already identified. Further, these systems have faint V_{peak} and have either no *Gaia* counterpart or have the *Gaia* counterpart with a near-zero parallax, so the *lack* of good data are confident signs that these systems are not disc novae. That is, any disc nova seen in the foreground of the bulge will be brighter than a bulge novae, which makes for a substantially great likelihood that *Gaia* will detect the counterpart and return a parallax that is significantly larger than 0.125 mas, and which makes for a substantially greater likelihood that the disc nova will have a distance measure from one of the old methods. While any high accuracy is impossible, I estimate a probability of 10 per cent or lower that a nova with no *Gaia* counterpart (and no distance measures from any of the old methods) is at a distance significantly closer than 8000 pc. The combination of these two probabilities gives ≥ 99.5 per cent that each individual remaining novae is a bulge system.

This probability estimate of ≥ 99.5 per cent has substantial uncertainties in its application. First, just because the expected number of disc nova interlopers is already overfilled does not mean that some small number of additional interlopers cannot be hiding amongst the poorly observed events. Second, a disc nova with a distance around 6000 pc could easily produce a *Gaia* counterpart whose parallax is too poor to be recognize as not being a bulge source, and such a nova could easily be too faint to trigger any of the various old methods to recognize its distance. Third, in the outer zones, I have not recognized the expected number of disc novae, so likely a few more unidentified disc interlopers are hiding around the edges of the bulge. Nevertheless, the basic probability result (that almost all of the novae in Table 4 not identified as “DISC” must be in the bulge population) is still confident, because the bulge-identifications are required to get the high numbers in the bulge component of Fig. 2. Therefore, the remaining non-DISC novae in Table 4 are almost all in the bulge population and are designated by ‘bulge’, with lower case letters.

Some novae do not neatly fit into the ‘bulge’ classification. These cases have population assignments of ‘disc’, ‘disc?’, and ‘bulge?’. Here are three examples to illustrate each of these population assignments: **(1)** KY Sgr has a parallax of -0.02 ± 0.10 mas, clearly indicating a distance comparable to D_{GC} . This nova has extinction of 0.55 mag (Shafter 1997) presumably from colors in quiescence, and 1.0 ± 0.5 mag from my fits to the spectral energy distribution (Schaefer 2022). The extinction along the entire line-of-sight is 3.29 mag (Schlafly & Finkbeiner 2011), while most of this must come from distances closer than the bulge (because with galactic latitude -1.72° the line-of-sight past the bulge is already far outside the disc). The discrepancy arises in trying to understand how KY Sgr can suffer much less than the maximum extinction, unless its distance is significantly closer than the 8000 pc. I do not know how to resolve this discrepancy, so I am labeling this system as ‘bulge?’. **(2)** Some of the novae have apparently contradictory information. For example, V630 Sgr has a parallax of 0.14 ± 0.11 mas pointing to a bulge distance (with parallax near 0.125 mas), yet has a well-observed peak with $V_{peak,0} = 2.2$ (implying a peak absolute magnitude of -12.3 for a galactic centre distance). In this case, I reconcile the two measures to a distance of 4000 pc, corresponding to a one-sigma deviation from the best-estimate parallax and corresponding to a peak absolute magnitude of -10.8 mag at the extreme end of the known distribution. I am labeling this as a ‘disc?’ nova. **(3)** The ‘disc’ novae are those with the measures pointing to the disc population, yet for which the evidence does not produce high confidence. FV Sct has a parallax of 0.48 ± 0.22 mas, for which the simple calculation gives a distance of 2000 pc, indicating a disc population. However, a parallax of 0.125 mas for bulge sources is only 1.6-sigma off the best-estimate parallax,

Table 5. *Gaia* Parallaxes and Magnitudes for 215 Galactic Novae (full table with 215 novae is in on-line supplementary material)

Nova	ϖ (mas)	b (mag)	g (mag)	r (mag)
OS And	0.21 ± 0.11	18.29	18.14	17.82
CI Aql	0.38 ± 0.04	16.43	15.79	14.94
DO Aql	0.35 ± 0.18	18.10	18.15	17.04
EL Aql	0.16 ± 0.08	18.10	16.59	15.42
EY Aql	-0.67 ± 0.70	21.05	20.20	19.12
...				
NQ Vul	0.84 ± 0.07	18.02	17.29	16.43
PW Vul	0.47 ± 0.08	17.85	17.66	17.21
QU Vul	1.11 ± 0.31	19.70	19.56	18.80
QV Vul	0.38 ± 0.18	18.87	18.56	17.86
V458 Vul	0.19 ± 0.11	18.30	18.10	17.80

so the parallax alone does not yield a decisive answer. The only other useful measure, $\mu_{peak} < 14.13 \pm 1.92$, is ambiguous, where the large error bars allow for both usual disc and bulge distances. I am labeling this case as ‘disc’ for the most likely population, but the lower case lettering indicates that this result is not of high confidence.

A minor question concerns the two novae that are inside globular clusters. Globular clusters are certainly in the older bulge (or halo) population, but the dynamical histories of these two novae are likely greatly different from the other bulge novae. I will dodge this question by assigning these to a separate “GlobC” population type.

In the end, many population assignments have good confidence as based on measured distances (the 38 ‘DISC’ and 86 ‘BULGE’ novae), most of the remainder have assignments with good confidence due to the requirement to get the large numbers of bulge novae as an excess above the disc component (the 75 ‘bulge’ novae), while a small fraction have assignments that are likely correct but individually of lesser confidence (the 4 ‘bulge?’, 9 ‘disc?’, and 2 ‘disc’ novae). Of the 214 novae in Table 4, 165 are identified as being in the bulge. The bulge fraction for all 402 known galactic novae is 41 per cent. This is the first list of bulge novae that I am aware of. And now, this list can be used for appropriate priors in the distance calculation.

5 GAIA DR3 PARALLAXES

On 2022 July 13, the *Gaia* Team released the much-anticipated Data Release 3 (DR3), with its impressive collection of parallaxes for stars down to roughly 19th magnitude and fainter from all over the sky. For the nova community, we finally have a collection of accurate and reliable distances for a large number of novae.

Gaia DR3 is part of a progression with great improvements in accuracy and number. Take the case of the brightest old novae, V603 Aql. Reported parallaxes are $\varpi = 4.011 \pm 0.137$ from *HST* (Harrison et al. 2013), 2.92 ± 0.54 mas from *Gaia* DR1 (Ramsay et al. 2017), 3.191 ± 0.069 mas from *Gaia* DR2 (Schaefer 2018), 3.11 ± 0.03 mas from *Gaia* EDR3, and now 3.106 ± 0.034 mas from *Gaia* DR3. The number of novae with accurate parallaxes progressed from 4 for *HST*, to 3 for DR1, 41 for DR2, and now 74 for DR3.

The *Gaia* spacecraft is described in Gaia Collaboration et al. (2016), while DR3 is described in Gaia Collaboration et al. (2022). DR3 data can be accessed from a European Space Agency website⁴.

A bureaucratic mode for extracting the *Gaia* parallaxes would be to run the standard search program and record the parallax for

the star nearest to the nova position. But this mindless approach would be bad for the majority of novae. One reason is that many dozens of novae have no identified quiescent counterpart, and no accurate position, so that the parallax for the *Gaia* star nearest to the cataloged nova position has likely no connection to the nova parallax. Another reason is that ~ 10 per cent of the faint novae have well-known counterparts that are more than one arc-second away from the catalogued positions, so a blind search would likely turn up the wrong answer. Further, many novae have a crowded field, such that many stars are close to the known nova position, so it is unclear as to which *Gaia* star is the real counterpart. A final problem is that many novae have the counterpart being faint, below the *Gaia* threshold, while the blind positional-coincidence method will then often take the meaningless parallax for a foreground star.

A proper use of the *Gaia* database for nova requires that some sort of a positive connection be made between the nova counterpart and the *Gaia* star. This connection can be made when the counterpart is known to be isolated to substantially fainter than the known counterpart magnitude, and the *Gaia* star is similarly isolated and of roughly the same magnitude as the counterpart. Further evidence might be that the *Gaia* star is relatively blue in color, or perhaps noted as a variable star. For the not-simple cases, I have used the *Gaia* catalog to construct a small star chart showing the relative positions and magnitudes, for direct comparison with a deep image on which the counterpart is positively identified. Excellent finder charts appear in the SMARTS catalog (Walter et al. 2012), the Duerbeck catalog (Duerbeck 1987), and the CVCat (Downes & Shara 2001). For purposes of this paper, I have included the *Gaia* parallax only when I can convince myself that the evidence is good for the *Gaia* star being the nova counterpart.

I have exhaustively searched for a confident *Gaia* counterpart for each of the 402 known galactic novae. In the majority of the cases, this has entailed making a star chart of the *Gaia* stars for comparison with picture of the real sky with tick marks identifying the counterpart or its location. For many other novae, the search consisted of seeing that *Gaia* recorded no stars within 2 arc-seconds of the nova position, and confirming in some other source that the *Gaia* position is the correct one. In 20 cases, *Gaia* DR3 reports on the nova counterpart, but no parallax is included. I have found a total of 195 nova parallaxes with DR3. From this, only 74 galactic novae have ‘good’ accuracy. Here ‘good’ accuracy is taken to be where the uncertainty on the parallax is < 0.30 times the parallax ($\sigma_{\varpi} < 0.30\varpi$), with this being the limit beyond which the prior contributes more to the final distance than does the new parallax information. For parallaxes with uncertainties from 0.30 to 1.0 times the parallax, I will label these measures as “poor”, for which my list has 66 novae. When $\sigma_{\varpi} > \varpi$, there is still marginal information, effectively just defining a lower limit on the nova distance, for which I have 55 novae from the DR3 catalog. Out of these near-zero parallaxes, 36 are actually negative parallaxes.

All of the 215 *Gaia* counterparts have their parallaxes and magnitudes reported in Table 5. The first column gives the nova name in the correct GCVS order, the second column gives the *Gaia* DR3 parallax in mas, and the last three columns give the *Gaia* magnitudes in the b , g , and r bands. To get distances in parsecs, these parallaxes must be combined with the priors from μ_{old} (see Table 1), μ_{peak} (see Table 3), and the population assignment (see Table 4).

⁴ <https://gea.esac.esa.int/archive/>

6 USING ALL THE INFORMATION TO GET THE BEST DISTANCES

The simple and traditional calculation of distance (D in parsecs) from a parallax (ϖ in mas with uncertainty σ_ϖ) is that $D = 1000/\varpi$ with an uncertainty of $\sigma_D = D * (\sigma_\varpi/\varpi)$. This is fine when the fractional error of the parallax is small. When the fraction error ($f=\sigma_\varpi/\varpi$) is not small, substantial problems arise (Bailer-Jones 2015). For $f \gtrsim 0.30$, the calculated probability distribution can become bimodal (where the results are telling us more about the prior information than about any new input), so the 30 per cent threshold is fine for recognizing parallaxes with good accuracy. To account for the non-linearities, the solution is to use a Bayesian calculation, as recommended by the *Gaia* Team (Luri et al. 2018). Detailed and helpful explanations and examples are given in Bailer-Jones (2015).

The *unnormalized* probability for the nova being at distance D , given the measured ϖ and σ_ϖ , is

$$P(D|\varpi, \sigma_\varpi) = P(\varpi|D, \sigma_\varpi) P(D). \quad (3)$$

The first factor on the right side of the equality is the probability that a nova at distance D will return a measured parallax of ϖ . The second factor on the right side is the ‘prior’, which encapsulates all previous knowledge of the nova distance. The first factor is

$$P(\varpi|D, \sigma_\varpi) = \frac{1}{\sigma_\varpi} \exp \left[-\frac{1}{2\sigma_\varpi^2} \left(\varpi - \frac{1}{D} \right)^2 \right]. \quad (4)$$

Throughout, the probability distributions can be multiplied by a normalization factor (i.e., the function integrated over all D) so that the integral of all the final probabilities is unity.

The prior information included in $P(D)$ can come from a variety of sources. Here, I will be including the information of the galactic position, the distance modulus from the old methods, and the distance modulus from V_{peak} . These are multiplicative, so

$$P(D) = P_{gal}(D|\ell, b) \times P_{old}(D|\mu_{old}) \times P_{peak}(D|\mu_{peak}). \quad (5)$$

The inclusion of these factors depends on the prior information for the nova, before and independent of the *Gaia* parallax.

The P_{gal} factor is representing the number of novae along a sightline as a function of distance, and this is the product of the nova space density as a function of distance times the volume of space in the expanding cone of the sightline. The P_{gal} factor depends on whether the nova is in the bulge or disc population. For a disc population,

$$P_{gal}(D) = D^2 \times \exp \left[\frac{-D \sin(|b|)}{\langle |Z| \rangle} \right] \times \exp \left[\frac{-R_{GC}}{h_R} \right]. \quad (6)$$

The D^2 factor represents the greater volume of space as we go to larger and larger distances. The first exponential factor represents the fact that disc populations have their number density decreasing exponentially with their vertical distance from the centre of the galactic plane, $Z=D\sin(b)$. Disc novae are observed to have an average value of $|Z|$, i.e., the exponential scale height $\langle |Z| \rangle$, for which I measure 140 pc (see Section 7.1). Along the line of sight towards a galactic latitude of b , the space number density of disc novae will fall off exponentially with distance. The exponential term involving the galactocentric distance, R_{GC} , is to represent the known exponential fall-off in star density of our Milky Way, with the scale length, h_R , roughly equal to 3000 pc. The value of R_{GC} is just a function of D , D_{GC} , and the galactic longitude ℓ . This representation of our galaxy does not incorporate any spiral arms or a bar in the centre. The exponential in R_{GC} has little effect on any distances, other than to cap the distances for poorly-observed disc novae at low galactic latitude. This formulation has suppressed constant factors, as these

all are absorbed into a normalization factor. This is the ‘exponentially decreasing space density’ (EDSD) prior (see equation 18 of Bailer-Jones 2015) recommended by the *Gaia* Team (Luri et al. 2018).

For a bulge novae, we can represent their radial distribution as a Gaussian along any line of sight with a central distance of D_{GC} and a one-sigma scatter of R_{bulge} . As a useable approximation for bulge novae, our prior information includes a Gaussian in D ;

$$P_{gal}(D) = D^2 \times \exp \left[-\frac{1}{2} \frac{(D - D_{GC})^2}{R_{bulge}^2} \right]. \quad (7)$$

Again, the D^2 factor covers the expanding volume at greater distances. I adopt $D_{GC}=8000$ pc and $R_{bulge}=750$ pc. All of the galactic novae will have the P_{gal} prior from either equation 6 or 7.

The prior information from the old methods and from V_{peak} have the distance moduli distributed as a Gaussian. For the prior based on the old methods,

$$P_{old}(D|\mu_{old}) = \exp \left[-\frac{1}{2} \frac{(5 \text{Log}[D] - 5 - \mu_{old})^2}{\sigma_{old}^2} \right]. \quad (8)$$

Many of the old measures from extinction are *lower limits*, and this can be handled by making the σ_{old} to be very large for any distance larger than the limit. In the closer direction, the quoted σ_{old} should be used as a reflection of the uncertainty in the value of the limit. Similarly, the prior for the distance information from V_{peak} will be

$$P_{peak}(D|\mu_{peak}) = \exp \left[-\frac{1}{2} \frac{(5 \text{Log}[D] - 5 - \mu_{peak})^2}{\sigma_{peak}^2} \right]. \quad (9)$$

Many novae only have faint limits on V_{peak} , or upper limits on μ_{peak} . This should be handled by setting σ_{peak} to the tabulated value for distances larger than the tabulated limit (to represent the uncertainty in the limit) or to a very large number for distances less than the tabulated limit (to represent the limit on the distance). With this, we can calculate the overall probability distribution for each nova, as a function of D and observed parameters.

This Bayesian formulation has a strong advantage that it provides a natural means to collect together all available information on D , where the old methods and the V_{peak} are correctly combined with the new *Gaia* parallaxes. The results are the best possible distances, taking into account all inputs. This is what I am presenting as the ‘Overall Best Distances’ in this paper’s title.

The calculated probability as a function of distance (from equation 3) should be normalized to an area under the curve of unity. (For display purposes, the probability curves are best normalized so that the peak probability is at unity, as then the shapes are not misperceived due to radical changes in the heights.) The resultant distribution functions always have an asymmetric and non-standard shape. (That is, the distributions are *not* Gaussians in distance.) These distributions record all the best information on D . However, presenting these distributions is awkward, and comparisons are hard. The solution is to extract from each distribution the most probable D and some range for representing the uncertainties. Following the recommendation of Bailer-Jones, I am using the mode of the probability distribution as the best estimator of D . That is, the D values I list will be for those at the maximum probability of the probability distribution. Further, to represent the reasonable range of D , I will not use the \pm notation (e.g., 1210^{+390}_{-220} pc), but will instead quote a range of D (e.g., 990–1600 pc). The range I chose to describe is that which contains the central 68 per cent of the probability distribution. The reason for choosing 68 per cent is because astronomers are practiced at knowing the meaning, whereas other choices would only be confusing.

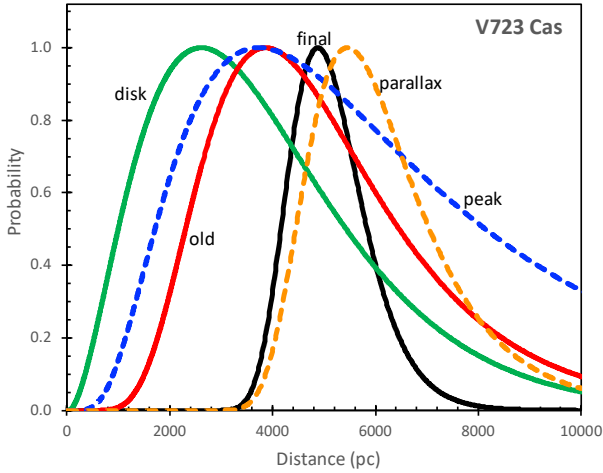


Figure 3. The probability distributions for V723 Cas. The final probability distribution is the unnormalized product of four separate probability distributions, each representing information on the distance to the nova. The P_{gal} distribution (solid green curve) represents the knowledge about the real distribution of novae in our galaxy, in this case for the space density of disc novae falling off exponentially with distance from the centre plane of our galaxy. The P_{old} distribution (solid red curve) represents the old measure of the expansion parallax as 3860 pc, with a real uncertainty of near 1690 pc. The P_{peak} distribution (dashed blue curve) is based on the observed peak magnitude of 7.10 ± 0.10 , the observed $E(B - V) = 0.40 \pm 0.10$, and the adopted average for all novae of $M_{V,peak}$ of -7.0 mag. The broad width of this distribution is because the one-sigma on the peak absolute magnitude being ± 1.4 mag. The $P(\varpi|D, \sigma_{\varpi})$ distribution (orange dashed curve) is from the *Gaia* DR3 parallax of 0.183 ± 0.035 mas. The $P(D|\varpi, \sigma_{\varpi})$ distribution (solid black curve) is the final best estimate of the probability of V723 Cas being at the given distance. This final curve is simply the product of the four input curves as displayed. (For display purposes only, the distributions have all been normalized so that the maximum probability is unity.) The narrowest of the four distributions is from the *Gaia* parallax, so the other three distributions serve only to push the distance somewhat closer. In the end, the best estimate of the distance to V723 Cas is that the highest point in the final curve is at 4880 pc, while the central 68 per cent of probability is inside the range 4390–5910 pc.

To illustrate this calculation (see Fig. 3), let me take the case of V723 Cas, as a typical nova with a moderate fraction error in the parallax ($f=0.19$), plus an old measure of the expansion parallax and a well measured peak magnitude. In Cassiopeia, the nova is certainly in the disc population and with a galactic latitude of b at -8.81° . Just given this galactic position, distances closer than 600 pc or so are unlikely simply because there is little volume inside this distance, while distances farther than 6000 pc or so are unlikely due to the nova then being required to be very far below the galactic centre plane. So just from the galactic position alone, the expected distance can be narrowed down to a range that is a factor of $10\times$ in size. For the old measures, we have an expansion parallax with a distance of 3860 pc, but the real uncertainty is much larger than published, as represented by the broad red curve in Fig. 3. For the P_{peak} information, the best estimate distance is 3730 pc as based on the peak magnitude alone. However, the ± 1.4 mag uncertainty on our adopted absolute means that the P_{peak} distributions will always be very broad. The *Gaia* parallax provides the best information, but even this is only accurate at the 19 per cent level. When all four of these distributions are multiplied together, the three non-parallax factors only serve to

push the final product to the near-side of the distribution allowed by the parallax. The parallax alone is pointing to distances centred on 5450 pc, but all three of the other sources of information are pointing to nearer distances, and these provide a weak pull on the parallax to produce a final distance of 4880 pc as the most probable value.

The resultant probability distributions are often roughly symmetric and similar to Gaussians in shape. But many novae have distributions that are substantially asymmetric. The most extreme cases are for FM Sgr and V1175 Sgr, their sharp peaks in the distribution (i.e., the mode) are outside the middle 68 per cent of the distribution.

I have calculated the best-estimate D values and the middle 68 per cent probability ranges for all 402 novae. These are presented in Table 6. I have a total of 220 novae with good accuracy in their distances. (For this, I take a ‘good’ distance to be one where half the quoted distance range is $\leq 0.3D$.) Out of these 219 novae with good distances, 52 are disc novae, with the primary basis for the accuracy being their *Gaia* parallaxes. The set of novae with good distances includes all 165 bulge novae. (These include only 20 novae with $\sigma_{\varpi} < 0.10$ mas, so the distance accuracy is almost entirely due to the identification as a bulge novae, with this being confident and reliable in all but a few marginal cases.) In addition the two novae in globular clusters have accurate *Gaia* parallaxes to the cluster. In the end, as the primary goal of my program, I have 220 novae (out of the 402 known galactic novae) that have accurate distances.

Table 6 also lists many of the fundamental measured properties for all 402 galactic novae. The first column gives the nova names, in the required GCVS order. The second column gives the year of the peak, or gives “RN” for recurrent novae. The third column gives the light curve classification according to the divisions of Strobe et al. (2010), consisting of one or two letters (S, P, PP, O, C, D, J, and F) plus the t_3 time (the number of days from the nova peak until the last time it fades below 3.0 mag under the peak) in parentheses. All of these classifications are from my own work with the original light curves for this paper. The fourth column gives the peak V-band magnitude, V_{peak} and its one-sigma uncertainty. These magnitudes are taken from my analysis of the original light curves, with the B-magnitudes converted to V-magnitudes, and care taken to identify when the peak was reliably detected. The fifth column gives the spectral class, with the main classes being Fe II, He/N, and hybrid, while neon-novae are indicated with an “Ne”. The next column gives the FWHM of the $H\alpha$ line in units of km/s, fairly early in the eruption. These data are often heterogeneous, with the only line width information coming from other hydrogen lines, or only the FWZI is quoted, or late in the eruption. The next column lists the 156 known orbital periods, P in days, as collected in Schaefer (2022), with this including my 49 new orbital periods. The eighth column gives my assignments for the nova population, as taken from Section 4. The ninth column gives my derived distances, D in parsecs, along with the range of the central 68 per cent of the probability distribution, with this column being the primary product of this paper. The tenth column gives the absolute magnitude at peak in the V-band, $M_{V,peak}$. These values are all calculated from the tabulated V_{peak} , $E(B - V)$, and D , with full extinction correction. The print copy of this table only shows the $M_{V,peak}$ values for those with uncertainties better than 1.0 mag. The on-line Supplementary Material has this column containing the measured values for all the novae, plus their formal one-sigma error bars. The last column gives a listing of the various unusual properties for each nova, with the notations keyed in a footnote to the table.

I have added a number of additional columns of measured properties, with these appearing only in the on-line Supplementary Material. Three of the columns give the galactic coordinates ℓ , b , and Θ_{GC} , all in units of degrees. The next column gives my final values for

Table 6. Distances and Properties of All 402 Known Galactic Novae (Supplementary Material has additional columns for ℓ , b , Θ_{GC} , $E(B - V)$, t_2 , and ϖ)

Nova	Year	LC(t_3)	V_{peak}	Spec.	FWHM	P	Pop.	D (68% range)	M_V	Properties ^a
OS And	1986.9	D(23)	6.50 ± 0.10	...	1740	...	DISC	4152 (3549 – 5349)	-7.06	...
CI Aql	RN	P(32)	9.00 ± 0.10	...	2250	0.61836	DISC	2761 (2555 – 3143)	-5.84	SubG, Ecl, ΔP , \dot{P}
DO Aql	1925.7	F(900)	8.50 ± 0.10	Fe II	...	0.16776	DISC	3151 (2571 – 4826)	-4.89	Ecl
EL Aql	1927.6	J(25)	5.32 ± 0.18	...	1230	...	DISC	4419 (3781 – 6450)	-10.91	...
EY Aql	1926.7	S(40)	9.69 ± 0.54	DISC	5819 (4214 – 9613)
V356 Aql	1936.7	J(140)	7.00 ± 0.10	Fe II	1140	0.42651	DISC	3243 (2668 – 5725)
V368 Aql	1936.8	S(42)	5.30 ± 0.20	Fe II	...	0.69051	DISC	2532 (2324 – 2948)	-8.58	SubG, Ecl
V500 Aql	1943.7	S(43)	6.13 ± 0.30	He/N	1400	0.14526	DISC	3291 (2655 – 4736)	-6.95	...
V528 Aql	1945.7	S(38)	6.90 ± 0.10	Fe II, Ne	915	...	DISC	2971 (2297 – 5479)
V603 Aql	1918.4	O(12)	-0.50 ± 0.10	Hybrid	...	0.13820	DISC	324 (320 – 327)	-8.30	Shell
V604 Aql	1905.7	S(25)	7.59 ± 0.25	...	1050	...	DISC	4631 (3508 – 7268)	-7.91	...
V606 Aql	1899.3	P	$<6.4 \pm 0.25$...	1280	...	DISC	3417 (2235 – 5688)	...	DN
V841 Aql	1951.5	...	$<9.9 \pm 1.02$	DISC	8178 (6238 – 13144)	...	DN
V1229 Aql	1970.3	P(32)	6.60 ± 0.10	Fe II	DISC	3317 (2734 – 4732)	-7.55	Shell
V1301 Aql	1975.4	S(85)	10.30 ± 0.30	He/N	1800	...	DISC	3537 (2852 – 5418)
V1370 Aql	1982.1	D(29)	7.70 ± 0.10	Ne	730	1.9581	DISC	3047 (2538 – 5209)	-5.80	SubG
V1378 Aql	1984.9	...	$<10.0 \pm 0.20$	DISC	3136 (2715 – 6142)
V1419 Aql	1993.4	D(32)	7.60 ± 0.10	DISC	4553 (3673 – 6276)	-7.24	...
V1425 Aql	1995.1	S(79)	8.00 ± 0.10	Fe II	1340	0.2558	DISC	3905 (2807 – 6884)	...	IP?
V1493 Aql	1999.5	C(50)	10.10 ± 0.10	...	3340	0.156	DISC	3948 (3120 – 5996)	-4.65	...
V1494 Aql	1999.9	O(16)	4.10 ± 0.10	Fe II, Ne	2470	0.13462	DISC	858 (784 – 1011)	-7.43	Ecl
V1548 Aql	2001.4	J	10.80 ± 0.30	Fe II	1100	...	DISC	7292 (5421 – 11337)
V1721 Aql	2008.7	...	$<14.0 \pm 0.20$	He/N	6450	...	DISC	7683 (5973 – 11366)
V1722 Aql	2010.0	S(16)	10.29 ± 0.10	Fe II	1000	...	DISC	7384 (5886 – 10477)	-8.70	...
V1723 Aql	2010.8	...	$<12.4 \pm 0.20$	Fe II	1500	...	DISC	8354 (5996 – 13512)
V1724 Aql	2012.9	...	12.00 ± 0.50	Fe II	950	...	DISC	6233 (4168 – 10328)
V1830 Aql	2013.9	...	15.20 ± 0.20	Fe II	1260	...	DISC	9166 (7411 – 13313)
V1831 Aql	2015.8	D	$<14.7 \pm 0.20$	Fe II	1350	...	DISC	7486 (5258 – 12917)
V2000 Aql	2020.5	...	$<15.6 \pm 0.20$	Fe II	2000	...	DISC	7480 (5046 – 11414)
V2029 Aql	2020.6	...	$<13.35 \pm 0.20$	Fe II	DISC	6795 (4446 – 10871)
V2030 Aql	2021.4	...	$<17.5 \pm 0.20$	He/N	2200	...	DISC	8979 (6410 – 15454)
OY Ara	1910.3	S(80)	5.77 ± 0.21	0.15539	DISC	2731 (2359 – 3795)	-7.40	Ecl
T Aur	1892.0	D(84)	4.50 ± 0.10	Fe II	...	0.20438	DISC	838 (815 – 870)	-6.42	Ecl, Shell
QZ Aur	1964.8	...	$<5.4 \pm 0.23$	0.35750	DISC	2478 (2212 – 3296)	...	Ecl, ΔP , \dot{P}
Z Cam	<c. 700	0.28984	DISC	214 (213 – 216)	...	DN
AT Cnc	c. 1686	...	$<3 \pm 0.20$	0.20163	DISC	465 (459 – 473)	...	DN
V435 CMa	2018.3	D(63)	9.90 ± 0.10	Fe II	1250	...	DISC	4079 (3069 – 6689)	-5.54	...
RS Car	1895.3	J(80)	7.10 ± 0.32	0.08244	DISC	5365 (3936 – 9265)	...	InGap, NonOrbP
V365 Car	1948.5	S(530)	9.29 ± 0.51	0.22369	DISC	2884 (2560 – 4362)
V679 Car	2008.9	S(24)	7.80 ± 0.10	Fe II	2000	...	DISC	6975 (5725 – 9652)	-8.28	...
V834 Car	2012.2	S(38)	10.20 ± 0.20	Fe II	1690	...	DISC	8897 (7363 – 11641)	-6.13	...
V906 Car	2018.3	J(64)	5.90 ± 0.20	Hybrid	325	...	DISC	3724 (2887 – 7554)
V919 Car	2014.4	...	$<10.1 \pm 0.20$	DISC	5338 (4106 – 8947)
V946 Car	2012.7	...	$<9.7 \pm 0.20$	DISC	3330 (2704 – 6650)
BC Cas	1929.6	...	$<9.7 \pm 0.63$	DISC	1896 (1742 – 2200)
V705 Cas	1993.9	D(67)	5.70 ± 0.10	Fe II	...	0.22828	DISC	2175 (2004 – 2491)	-7.26	Shell
V723 Cas	1995.6	J(299)	7.10 ± 0.10	Fe II, Ne	600	0.69327	DISC	4622 (4183 – 5482)	-7.46	SubG, V1500, Sh
V1391 Cas	2020.7	D(120)	10.60 ± 0.10	Fe II	DISC	3784 (2789 – 6750)
V1405 Cas	2021.3	J(175)	5.20 ± 0.10	Hybrid	...	0.18839	DISC	1809 (1630 – 1848)	-7.79	γ
MT Cen	1931.4	D(10)	7.74 ± 0.23	...	910	...	DISC	5260 (3892 – 9442)
V812 Cen	1973.3	...	$<10.4 \pm 0.23$	Fe II	1800	...	DISC	4118 (3022 – 7230)
V842 Cen	1986.9	D(48)	4.90 ± 0.10	Fe II	760	...	DISC	1372 (1300 – 1472)	-7.65	Shell, IP?
V868 Cen	1991.3	J(82)	8.70 ± 0.10	Fe II	700	...	DISC	3890 (3034 – 6122)	-9.67	...
V888 Cen	1995.1	O(90)	8.00 ± 0.10	Fe II	DISC	2937 (2681 – 3459)	-5.39	...
V1039 Cen	2001.7	J(174)	9.30 ± 0.10	0.247	DISC	3483 (2776 – 6748)	...	IP?
V1047 Cen	2005.6	P(26)	8.50 ± 0.20	Fe II	840	...	DISC	4174 (3295 – 6463)	-7.70	Rebrighten(2019)
V1065 Cen	2007.1	P(26)	6.60 ± 0.20	Fe II, Ne	2700	...	DISC	3322 (2687 – 4980)	-7.46	...
V1213 Cen	2009.3	S(30)	8.50 ± 0.10	Fe II	2300	0.21201	DISC	5437 (4575 – 7587)	-7.97	DN
V1368 Cen	2012.3	P(34)	9.40 ± 0.10	Fe II	1140	...	DISC	6345 (5168 – 8539)
V1369 Cen	2014.0	D(65)	3.30 ± 0.10	Fe II	408	0.15656	DISC	643 (531 – 1048)	-6.08	γ
V1375 Cen	2010.6	...	$<10.3 \pm 0.20$...	1400	0.3604	DISC	1042 (1005 – 1087)
V1404 Cen	2015.2	S	$<10.7 \pm 0.20$	DISC	7800 (6088 – 12341)
V1405 Cen	2017.4	J(115)	10.90 ± 0.30	Fe II	1600	...	DISC	7058 (5311 – 11759)

Table 6 – *continued* Distances and Properties of All 402 Known Galactic Novae

Nova	Year	LC(t_3)	V_{peak}	Spec.	FWHM	P	Pop.	D (68% range)	M_V	Properties ^a
IV Cep	1971.5	S(37)	7.00 ± 0.40	Fe II	DISC	6463 (5632 – 9009)	-9.07	...
V809 Cep	2013.2	D(36)	11.18 ± 0.10	Fe II	500	...	DISC	6162 (5051 – 10594)
V962 Cep	2014.3	S(42)	11.00 ± 0.10	Fe II	2000	...	DISC	5545 (4606 – 7262)	-5.63	...
HV Cet	2008.8	...	$<14.2 \pm 0.20$	Ne	2900	1.7718	DISC	380 (260 – 881)	...	SubG, PreERise
RR Cha	1953.3	...	$<6.7 \pm 0.25$	0.1401	DISC	1860 (1615 – 2628)	...	Ecl
X Cir	1927.0	...	$<6.1 \pm 0.25$...	1420	0.15446	DISC	3267 (2144 – 5718)	...	Ecl
AR Cir	1906.1	J(330)	8.29 ± 0.45	0.2143	DISC	1456 (1306 – 1842)
BY Cir	1995.1	P(124)	7.40 ± 0.10	Fe II	1500	0.2816	DISC	2396 (2078 – 3347)	...	Ecl
DD Cir	1999.6	P(16)	7.60 ± 0.10	0.09746	DISC	3244 (2410 – 5328)	-6.26	InGap, Ecl, IP?
DE Cir	2003.8	S(4)	7.70 ± 0.50	He/N	5100	...	DISC	6153 (5236 – 8583)
FM Cir	2018.1	J(85)	5.90 ± 0.20	Fe II	1500	0.14977	DISC	3245 (2751 – 5043)	-7.37	...
V394 CrA	RN	P(5)	7.20 ± 0.10	...	4600	1.51568	BULGE	7662 (6931 – 8405)	-7.84	SubG, Ecl, \dot{P}
V655 CrA	1967.5	...	$<7.7 \pm 0.23$	BULGE	8212 (7529 – 8975)
V693 CrA	1981.3	S(18)	7.00 ± 0.10	Ne	4500	...	BULGE	8027 (7300 – 8733)	-7.83	...
T CrB	RN	S(6)	2.50 ± 0.10	...	4980	227.532	DISC	914 (892 – 938)	-7.62	RG, PreERise, ΔP , \dot{P}
AP Cru	1935.2	...	$<9.9 \pm 0.23$	DISC	5632 (4615 – 9793)
CP Cru	1996.7	...	$<9.2 \pm 0.20$	He/N, Ne	2000	0.944	DISC	2402 (1949 – 3879)	...	SubG, Ecl
V450 Cyg	1942.7	D(108)	7.80 ± 0.30	Fe II	DISC	4587 (4077 – 5690)	-6.78	...
V465 Cyg	1948.4	...	9.49 ± 0.50	Fe II	DISC	5487 (4207 – 8475)
V476 Cyg	1920.6	D(16)	1.90 ± 0.10	Fe II	DISC	1179 (1078 – 1377)	-9.02	Shell
V1330 Cyg	1970.4	S	$<8.5 \pm 0.23$	0.50	DISC	2883 (2557 – 3976)
V1500 Cyg	1975.7	S(4)	1.90 ± 0.10	Hybrid, Ne	...	0.13962	DISC	1504 (1343 – 1823)	-10.38	V1500, AP, PreERise, Sh
V1668 Cyg	1978.7	S(26)	6.20 ± 0.10	Fe II, Ne	2400	0.1384	DISC	3836 (3144 – 5247)	-7.90	Ecl
V1819 Cyg	1986.6	J(181)	9.30 ± 0.10	Fe II	2742	...	DISC	6428 (5219 – 8877)	-6.29	Shell
V1974 Cyg	1992.1	P(43)	4.30 ± 0.10	Hybrid, Ne	2000	0.08126	DISC	1618 (1510 – 1796)	-7.55	InGap, V1500, Sh
V2274 Cyg	2001.5	D(33)	11.50 ± 0.10	Fe II	950	...	DISC	7227 (5755 – 10379)	-6.92	...
V2275 Cyg	2001.6	S(8)	6.90 ± 0.10	...	2100	0.31449	DISC	3302 (2771 – 4930)	-8.79	...
V2361 Cyg	2005.1	S(8)	10.20 ± 0.20	He/N	2200	...	DISC	5492 (4393 – 8096)	-7.22	...
V2362 Cyg	2006.3	C(246)	8.10 ± 0.10	Fe II	1850	...	DISC	5438 (4461 – 8717)	-7.31	...
V2467 Cyg	2007.2	O(20)	7.40 ± 0.10	Fe II	950	0.15379	DISC	1836 (1637 – 2360)	-8.26	...
V2468 Cyg	2008.0	S(20)	7.60 ± 0.40	Hybrid	2100	0.14525	DISC	5983 (4719 – 9073)	-8.70	...
V2491 Cyg	2008.3	C(16)	7.50 ± 0.10	He/N	4860	...	DISC	4786 (4101 – 6339)	-6.61	IP?
V2659 Cyg	2014.3	J(140)	9.30 ± 0.10	Fe II	1000	...	DISC	5384 (4725 – 6780)	-6.53	...
V2891 Cyg	2019.8	J	14.30 ± 0.20	Fe II	820	...	DISC	6991 (4850 – 13752)
Q Cyg	1876.9	S(11)	3.00 ± 0.10	Fe II	...	0.42036	DISC	663 (658 – 669)	-6.91	...
HR Del	1967.5	J(231)	3.60 ± 0.10	Fe II, Ne	...	0.21416	DISC	897 (880 – 915)	-6.50	ΔP , \dot{P} , Sh
V339 Del	2013.7	PP(29)	4.80 ± 0.10	Fe II	1421	0.16294	DISC	1587 (1288 – 2925)	-6.76	γ
KT Eri	RN	PP(14)	5.42 ± 0.02	He/N	3300	2.61595	DISC	4211 (3915 – 4677)	-7.95	SubG, LAmpVar
DM Gem	1903.2	S(22)	4.78 ± 0.21	DISC	3289 (2868 – 4298)	-8.15	...
DN Gem	1912.2	P(35)	3.60 ± 0.10	Fe II	...	0.12784	DISC	1381 (1300 – 1511)	-7.63	...
DQ Her	1934.9	D(100)	1.60 ± 0.10	Fe II, Ne	...	0.19362	DISC	496 (492 – 500)	-7.03	Ecl, ΔP , \dot{P} , IP, Sh
V446 Her	1960.2	S(11)	2.52 ± 0.10	He/N	...	0.207	DISC	1256 (1176 – 1386)	-9.12	DN, Shell
V533 Her	1963.1	S(43)	3.00 ± 0.10	Fe II	...	0.147	DISC	1269 (1236 – 1307)	-7.61	IP?, Sh, PreERise
V827 Her	1987.1	S(53)	7.50 ± 0.10	DISC	2366 (1894 – 4325)
V838 Her	1991.2	P(4)	5.30 ± 0.10	He/N, Ne	5000	0.29764	DISC	3128 (2657 – 4164)	-8.73	Ecl
V1674 Her	2021.5	S(2)	6.20 ± 0.20	0.15302	DISC	3216 (2472 – 5359)	...	IP, γ
CP Lac	1936.5	S(9)	2.00 ± 0.10	Hybrid	...	0.14514	DISC	1164 (1125 – 1205)	-9.17	Shell
DI Lac	1911.0	S(43)	4.23 ± 0.40	Fe II	DISC	1729 (1682 – 1786)	-7.77	...
DK Lac	1950.1	J(202)	5.90 ± 0.10	Fe II	DISC	2986 (2700 – 3604)	-7.34	Shell
HY Lup	1993.7	S(26)	7.70 ± 0.50	Fe II	2700	...	DISC	2281 (1826 – 3446)	-5.08	...
PR Lup	2011.7	J(40)	8.60 ± 0.20	Fe II	1700	...	DISC	6715 (5577 – 8851)	-7.40	...
V407 Lup	2016.8	S(8)	6.40 ± 0.20	Fe II	3700	3.62	DISC	2900 (2281 – 4724)	-6.78	SubG, IP?, NonOrbP, γ
V408 Lup	2018.5	J(87)	8.98 ± 0.10	Fe II	1300	...	DISC	4550 (3307 – 7045)
HR Lyr	1919.9	...	6.50 ± 0.50	Fe II	...	0.90578	DISC	4704 (4305 – 5447)	-7.36	SubG
BT Mon	1940.0	F(182)	8.10 ± 0.10	...	2100	0.33381	DISC	1580 (1513 – 1668)	-3.64	Ecl, ΔP , \dot{P} , Sh
GI Mon	1918.1	S(23)	5.39 ± 0.50	He/N	...	0.44706	DISC	3357 (3038 – 4076)	-7.55	Ecl, DN, IP?
KT Mon	1942.9	S(40)	9.64 ± 0.41	He/N	DISC	5048 (3793 – 8343)
V959 Mon	2012.7	S	$<9.4 \pm 0.20$	Ne	...	0.29585	DISC	2902 (2485 – 4070)	...	γ
GQ Mus	1983.0	P(108)	7.80 ± 0.30	...	1000	0.05937	DISC	4043 (3248 – 6447)	-6.63	<Gap, V1500
LZ Mus	1999.0	P(12)	8.50 ± 0.10	DISC	6749 (5751 – 9332)	-8.59	...
QY Mus	2008.7	D(100)	8.60 ± 0.20	Fe II	1550	0.90114	DISC	4570 (3886 – 6053)	-6.53	SubG, NonOrbP
V357 Mus	2018.1	D(32)	6.70 ± 0.10	0.15516	DISC	2991 (2544 – 5074)
IL Nor	1893.5	S	6.34 ± 0.15	0.06709	DISC	3318 (2404 – 5886)	...	<Gap

Table 6 – continued Distances and Properties of All 402 Known Galactic Novae

Nova	Year	LC(t_3)	V_{peak}	Spec.	FWHM	P	Pop.	D (68% range)	M_V	Properties ^a
IM Nor	RN	P(80)	8.50 ± 0.10	...	2380	0.20717	DISC	4312 (3461 – 6326)	-7.15	Ecl, \dot{P}
V341 Nor	1983.7	S(14)	9.40 ± 0.50	...	3000	...	DISC	7436 (5476 – 11209)
V382 Nor	2005.2	S(18)	8.70 ± 0.40	Fe II	1850	...	DISC	5615 (4341 – 8119)	-7.68	...
V390 Nor	2007.5	J	9.10 ± 0.30	Fe II	...	0.17133	DISC	4174 (3337 – 6010)	-6.79	...
V555 Nor	2016.3	S(110)	12.70 ± 0.40	He/N	2140	...	DISC	7561 (5476 – 11720)
V556 Nor	2018.9	S(9)	10.10 ± 0.40	Fe II	2800	...	DISC	5840 (4028 – 9161)
RS Oph	RN	P(14)	4.80 ± 0.10	...	3930	453.6	DISC	2710 (2575 – 2908)	-9.63	RG, γ , PostEdip
BB Oph	1897.4	...	$<11.3 \pm 0.20$	bulge	8142 (7396 – 8883)
V553 Oph	1940.6	...	11.06 ± 0.58	BULGE	8124 (7394 – 8871)
V794 Oph	1939.5	J(220)	10.69 ± 0.41	18	BULGE	8463 (7765 – 9179)	-6.74	RG
V840 Oph	1917.3	...	6.04 ± 0.52	bulge	7975 (7231 – 8720)	-9.55	...
V841 Oph	1848.3	J(130)	4.30 ± 0.40	0.60130	DISC	843 (831 – 857)	-6.57	SubG
V849 Oph	1919.6	F(270)	7.60 ± 0.10	Fe II, Ne	...	0.17276	DISC	3637 (3007 – 5127)	-5.51	Ecl
V906 Oph	1952.6	...	8.54 ± 0.39	Fe II	2000	...	bulge	8079 (7344 – 8826)	-8.01	...
V908 Oph	1954.5	...	$<7.9 \pm 0.36$	disc?	4931 (3139 – 7833)
V972 Oph	1957.7	J(176)	7.39 ± 0.23	0.27964	DISC	778 (691 – 1111)	-3.62	...
V1012 Oph	1961.3	...	$<12.9 \pm 0.45$	BULGE	8124 (7396 – 8883)
V2024 Oph	1967.5	...	$<10.2 \pm 0.36$	bulge	8137 (7396 – 8883)
V2104 Oph	1976.7	...	$<8.8 \pm 0.20$	He/N, Ne	870	...	DISC	1691 (1315 – 3115)
V2109 Oph	1969.5	...	$<9.8 \pm 0.36$	1.32379	BULGE	8138 (7398 – 8873)	...	SubG, DN
V2214 Oph	1988.3	S(89)	8.50 ± 0.10	Fe II, Ne	1025	0.11752	BULGE	7990 (7328 – 8708)	-8.03	...
V2264 Oph	1991.3	S(30)	10.00 ± 0.10	Fe II, Ne	2300	...	bulge	8155 (7417 – 8893)	-6.73	...
V2290 Oph	1991.3	...	$<9.3 \pm 0.20$	bulge	8149 (7395 – 8882)
V2295 Oph	1993.3	F(16)	9.30 ± 0.10	Fe II	bulge	8097 (7366 – 8844)	-7.57	...
V2313 Oph	1994.4	S(17)	7.50 ± 0.10	Fe II	2500	...	disc?	2738 (2126 – 5592)
V2487 Oph	RN	P(8)	9.50 ± 0.10	...	10000	1.24	BULGE	7539 (6812 – 8282)	-6.44	SubG, Superflare
V2540 Oph	2002.1	J(115)	8.10 ± 0.10	0.28478	BULGE	8117 (7389 – 8859)	-7.66	Ecl
V2573 Oph	2003.5	D(81)	10.60 ± 0.10	Fe II	1300	...	bulge	8149 (7416 – 8890)	-6.81	...
V2574 Oph	2004.3	S(41)	10.20 ± 0.30	Fe II	1500	0.13509	BULGE	8157 (7415 – 8888)	-7.09	NonOrbP
V2575 Oph	2006.1	J(66)	11.00 ± 0.40	Fe II	560	...	DISC	4055 (3307 – 5480)	-6.38	...
V2576 Oph	2006.3	S(29)	9.20 ± 0.40	Fe II	1470	...	DISC	2968 (2341 – 4798)	-5.08	...
V2615 Oph	2007.2	S(48)	8.50 ± 0.30	Fe II	800	0.27234	DISC	2529 (2018 – 4398)
V2670 Oph	2008.4	J(37)	10.00 ± 0.40	Fe II	600	...	BULGE	7825 (7111 – 8560)	-7.26	...
V2671 Oph	2008.4	...	11.10 ± 0.10	Fe II	1210	...	BULGE	8150 (7432 – 8905)	-6.56	...
V2672 Oph	2009.6	S(6)	10.10 ± 0.40	He/N	8000	...	BULGE	7703 (6967 – 8447)	-9.29	...
V2673 Oph	2010.1	S(28)	8.30 ± 0.10	Fe II	bulge	8042 (7296 – 8778)	-8.43	...
V2674 Oph	2010.2	S(31)	9.25 ± 0.10	Fe II	1650	1.30207	DISC	3204 (2519 – 5295)	...	SubG, Ecl
V2676 Oph	2012.3	D(68)	10.60 ± 0.10	Fe II	950	...	BULGE	8149 (7438 – 8864)	-6.78	...
V2677 Oph	2012.5	S(13)	10.80 ± 0.20	Fe II	3000	0.34430	bulge	8174 (7463 – 8888)	-7.79	...
V2944 Oph	2015.3	J(145)	9.00 ± 0.20	Hybrid	1050	...	BULGE	8285 (7626 – 8988)	-7.45	...
V2949 Oph	2015.9	J	11.90 ± 0.40	Fe II	900	...	BULGE	8365 (7668 – 9101)
V3661 Oph	2016.3	S(5.7)	10.79 ± 0.20	Fe II	1200	...	bulge	7873 (7126 – 8624)	-11.13	...
V3662 Oph	2017.4	...	$<13.6 \pm 0.20$	Fe II	1400	...	bulge	8125 (7396 – 8883)
V3663 Oph	2017.9	...	$<9.4 \pm 0.20$	Fe II	2500	...	bulge	8081 (7344 – 8827)
V3664 Oph	2018.2	...	$<12.8 \pm 0.20$	Fe II	...	2250	bulge	8129 (7376 – 8867)	...	RG
V3665 Oph	2018.3	S(61)	9.30 ± 0.50	Fe II	1400	...	bulge	8136 (7406 – 8881)	-6.96	...
V3666 Oph	2018.7	S(57)	9.50 ± 0.20	Fe II	930	...	DISC	1701 (1605 – 5260)
V3701 Oph	2010.8	...	$<11.2 \pm 0.20$	bulge	8104 (7365 – 8848)
V3730 Oph	2019.8	...	$<12.3 \pm 0.20$...	3000	...	BULGE	8072 (7336 – 8821)
V3731 Oph	2019.6	...	$<13.3 \pm 0.20$	He/N	2600	...	bulge	8129 (7378 – 8857)
V3732 Oph	2021.2	...	$<15.8 \pm 0.20$	He/N	1800	0.94004	bulge	8136 (7396 – 8883)	...	SubG
Nova 1938 Oph	1938.5	...	$<15.1 \pm 0.23$	GlobC	8652 (8122 – 9157)	...	in M14
V2860 Ori	2019.7	P(13)	10.00 ± 0.20	He/N	4000	0.42258	DISC	5969 (4698 – 9275)	-5.43	...
V Per	1888.0	...	$<8.7 \pm 0.25$	0.10712	DISC	3152 (2687 – 5304)	...	InGap, Ecl
GK Per	1901.1	O(13)	0.20 ± 0.10	Fe II, Ne	...	1.99680	DISC	434 (427 – 442)	-9.04	SubG, DN, IP, Sh
V392 Per	2018.4	P(11)	6.20 ± 0.10	Ne	...	3.21997	DISC	3402 (3071 – 4178)	-10.12	SubG, DN, γ
V400 Per	1974.9	J(110)	8.00 ± 0.40	He/N	...	0.82639	DISC	3222 (2543 – 4946)	-5.04	SubG
V1112 Per	2021.0	D(34)	8.20 ± 0.10	Fe II	1550	...	DISC	3945 (3055 – 6706)	-6.80	...
RR Pic	1925.4	J(122)	1.00 ± 0.10	Fe II	...	0.14502	DISC	501 (496 – 507)	-7.69	ΔP , \dot{P} , Sh
CP Pup	1942.9	P(8)	0.70 ± 0.10	He/N	...	0.06126	DISC	783 (770 – 793)	-9.39	<Gap, V1500, Sh
DY Pup	1902.9	...	$<6.7 \pm 0.23$	0.13952	DISC	3585 (2791 – 6051)	...	Ecl
HS Pup	1963.9	S(65)	7.37 ± 0.23	0.17864	DISC	4637 (3909 – 7380)	-7.57	...
HZ Pup	1963.0	J(70)	7.24 ± 0.18	0.212	DISC	2899 (2615 – 3639)	-6.16	IP

Table 6 – *continued* Distances and Properties of All 402 Known Galactic Novae

Nova	Year	LC(t_3)	V_{peak}	Spec.	FWHM	P	Pop.	D (68% range)	M_V	Properties ^a
V351 Pup	1992.0	P(26)	6.40 ± 0.10	Fe II, Ne	...	0.1182	DISC	3869 (3077 – 5996)	-8.55	Shell
V445 Pup	2000.9	D(240)	8.60 ± 0.10	Helium	DISC	6272 (5026 – 9026)	-6.97	Shell
V574 Pup	2004.9	S(27)	7.00 ± 0.10	Fe II, Ne	2830	...	DISC	4567 (3744 – 7174)	-7.85	...
V597 Pup	2007.6	S(6)	6.20 ± 0.50	Hybrid	1800	0.11119	DISC	5851 (4682 – 9384)	-8.57	Ecl, IP?
V598 Pup	2007.6	...	$<10.2 \pm 0.20$	He/N	2100	0.16287	DISC	1844 (1755 – 1965)	...	NonOrbP
T Pyx	RN	P(62)	6.40 ± 0.10	Hybrid	5350	0.07623	DISC	3599 (3369 – 3931)	-7.16	InGap, Ecl, ΔP , \dot{P} , PreERise, V1500, Sh
YZ Ret	2020.6	P(22)	3.70 ± 0.40	He/N, Ne	2500	0.13245	DISC	2388 (2234 – 2636)	-8.25	NonOrbP, γ
WY Sge	1783.6	...	$<6 \pm 0.20$	0.15363	DISC	1069 (983 – 1264)	...	Ecl, DN?
HS Sge	1977.0	P(21)	7.20 ± 0.10	...	1600	...	DISC	3193 (2403 – 6432)
AT Sgr	1900.7	...	$<9.4 \pm 1.12$	disc?	7776 (4602 – 10006)
BS Sgr	1917.5	...	$<8.8 \pm 0.23$...	640	...	BULGE	8216 (7530 – 8937)
FL Sgr	1924.4	...	$<7.9 \pm 0.25$	bulge	8094 (7364 – 8842)
FM Sgr	1926.5	...	$<7.9 \pm 0.29$	DISC	653 (740 – 6269)
GR Sgr	1924.3	...	$<11.0 \pm 0.23$	29.4956	DISC	1406 (1325 – 1530)	...	RG
HS Sgr	1900.7	...	$<10.8 \pm 0.29$	BULGE	8143 (7391 – 8879)
KY Sgr	1926.4	S(109)	9.94 ± 0.36	294	bulge?	7801 (7084 – 8534)	-6.23	RG
V363 Sgr	1927.7	...	$<8.6 \pm 0.21$...	685	0.12607	BULGE	8141 (7395 – 8884)
V441 Sgr	1930.7	...	$<8.2 \pm 0.25$	bulge	8098 (7364 – 8841)
V630 Sgr	1936.8	S(11)	3.49 ± 0.29	Ne	...	0.11793	disc?	3595 (3068 – 5469)	-10.53	Ecl
V726 Sgr	1936.3	S(95)	10.04 ± 0.34	Ne	...	0.82281	BULGE	8245 (7511 – 8976)	-5.63	SubG
V732 Sgr	1936.4	D(75)	6.40 ± 0.10	DISC	3251 (2551 – 5741)
V787 Sgr	1937.4	...	$<9.2 \pm 0.25$	BULGE	8186 (7456 – 8933)
V909 Sgr	1941.5	...	6.49 ± 0.52	Ne	...	0.14286	bulge	8036 (7291 – 8776)	-8.66	Ecl
V927 Sgr	1944.3	...	$<7.6 \pm 0.23$	BULGE	8065 (7323 – 8803)
V928 Sgr	1947.4	...	$<8.4 \pm 0.23$	Fe II	690	...	bulge	8107 (7378 – 8854)
V990 Sgr	1936.7	S(24)	10.09 ± 0.50	BULGE	8224 (7507 – 8953)
V999 Sgr	1910.2	J(160)	7.41 ± 0.29	...	595	0.15184	DISC	3122 (2780 – 4905)	-6.86	...
V1012 Sgr	1914.6	...	7.59 ± 0.54	BULGE	8072 (7323 – 8805)	-7.87	...
V1014 Sgr	1901.4	...	10.07 ± 0.54	bulge	8142 (7419 – 8894)	-6.72	...
V1015 Sgr	1905.6	...	$<6.7 \pm 0.25$	BULGE	8012 (7267 – 8751)
V1016 Sgr	1899.8	...	$<8.0 \pm 0.23$	13.4	DISC	2666 (2538 – 2844)	...	RG, NonOrbP, IP?
V1017 Sgr	1919.2	...	$<6.8 \pm 0.23$	5.78629	DISC	1226 (1194 – 1264)	...	SubG, DN, ΔP , \dot{P}
V1059 Sgr	1898.2	S(26)	4.54 ± 0.62	0.2861	DISC	2694 (2379 – 3708)	-8.39	...
V1148 Sgr	1943.6	...	$<7.3 \pm 0.29$	DISC	2148 (2009 – 2377)
V1149 Sgr	1945.1	...	$<7.0 \pm 0.23$...	960	...	BULGE	8080 (7343 – 8816)
V1150 Sgr	1946.4	...	$<12.6 \pm 0.25$	BULGE	8126 (7396 – 8883)
V1151 Sgr	1947.3	...	$<10.2 \pm 0.29$	bulge	8145 (7394 – 8878)
V1172 Sgr	1951.2	...	$<8.5 \pm 0.25$...	2500	255	BULGE	7512 (6825 – 8254)	...	RG
V1174 Sgr	1952.2	...	$<11.2 \pm 0.29$	0.30905	bulge	8141 (7396 – 8883)
V1175 Sgr	1952.1	...	$<6.7 \pm 0.23$	disc?	1275 (1339 – 5400)
V1275 Sgr	1954.5	...	$<6.6 \pm 0.25$...	1000	...	BULGE	7958 (7235 – 8695)
V1310 Sgr	1935.4	F(390)	11.44 ± 0.15	BULGE	8375 (7647 – 9102)	-3.64	...
V1572 Sgr	1955.1	...	$<10.3 \pm 0.25$	bulge	8136 (7396 – 8883)
V1583 Sgr	1928.6	S(37)	8.29 ± 0.36	...	780	...	BULGE	8098 (7360 – 8841)
V1944 Sgr	1960.4	...	$<10.9 \pm 0.54$	disc?	7766 (4786 – 9653)
V2415 Sgr	1951.7	...	$<12.0 \pm 0.36$	bulge	8141 (7396 – 8883)
V2572 Sgr	1969.5	S(44)	6.26 ± 0.50	0.15704	BULGE	8065 (7329 – 8802)	-8.68	...
V3645 Sgr	1970.6	...	$<12.1 \pm 0.23$	39.5	BULGE	7581 (6847 – 8342)	...	RG
V3888 Sgr	1974.8	...	$<9.0 \pm 0.20$	Fe II	BULGE	7696 (6955 – 8432)
V3889 Sgr	1975.5	...	$<8.4 \pm 0.20$	BULGE	8094 (7363 – 8837)
V3890 Sgr	RN	S(14)	8.10 ± 0.10	Hybrid	2140	747.6	BULGE	8546 (8097 – 9058)	-8.39	RG, γ
V3964 Sgr	1975.4	...	$<8.8 \pm 0.29$	Fe II	1320	...	BULGE	8129 (7388 – 8862)
V4021 Sgr	1977.2	P(215)	8.90 ± 0.10	BULGE	8177 (7439 – 8909)	-6.59	...
V4027 Sgr	1968.4	...	$<10.3 \pm 0.29$	Fe II	2900	...	BULGE	8353 (7648 – 9085)
V4049 Sgr	1978.2	...	$<12.0 \pm 0.20$	Fe II	BULGE	8135 (7396 – 8883)
V4065 Sgr	1980.8	...	$<9.0 \pm 0.20$	BULGE	7863 (7219 – 8561)
V4077 Sgr	1982.8	J	8.00 ± 0.40	Fe II	BULGE	7610 (6864 – 8351)	-7.40	...
V4092 Sgr	1984.7	...	$<10.5 \pm 0.20$	bulge	8115 (7377 – 8857)
V4121 Sgr	1983.1	...	$<9.5 \pm 0.20$	BULGE	8135 (7396 – 8883)
V4135 Sgr	1987.4	...	10.40 ± 0.40	...	1000	...	BULGE	8178 (7454 – 8925)	-6.33	...
V4157 Sgr	1992.1	S(7)	7.00 ± 0.50	Fe II	1800	...	bulge	7946 (7201 – 8694)	-10.29	...
V4160 Sgr	1991.6	S(3)	7.00 ± 0.10	He/N, Ne	4500	...	DISC	2602 (2062 – 4091)	-6.07	...

Table 6 – continued Distances and Properties of All 402 Known Galactic Novae

Nova	Year	LC(t_3)	V_{peak}	Spec.	FWHM	P	Pop.	D (68% range)	M_V	Properties ^a
V4160 Sgr	1991.6	S(3)	7.00 ± 0.10	He/N, Ne	4500	...	DISC	2602 (2062 – 4091)	-6.07	...
V4169 Sgr	1992.5	S(36)	7.90 ± 0.10	Fe II	DISC	2939 (2322 – 4561)	-5.49	...
V4171 Sgr	1992.8	S(20)	6.60 ± 0.20	Fe II	1200	...	bulge	7946 (7206 – 8697)	-9.76	...
V4327 Sgr	1993.6	S(30)	8.10 ± 0.30	Hybrid	2400	...	bulge	8092 (7359 – 8837)	-7.62	...
V4338 Sgr	1990.1	...	8.00 ± 0.50	...	400	29.48192	BULGE	8117 (7399 – 8853)	-8.41	RG
V4361 Sgr	1996.5	...	$<10.3 \pm 0.20$	Fe II	DISC	6845 (4332 – 9474)
V4362 Sgr	1994.4	D(121)	7.80 ± 0.20	Fe II	450	...	bulge	8074 (7344 – 8828)
V4444 Sgr	1999.3	S(9)	7.60 ± 0.10	Fe II	800	...	BULGE	7595 (6870 – 8360)	-8.20	...
V4579 Sgr	1986.8	...	$<10.4 \pm 0.20$	0.15356	DISC	1372 (1304 – 1467)	...	Ecl
V4633 Sgr	1998.2	P(44)	7.40 ± 0.10	Fe II	1700	0.12557	disc	2426 (1917 – 3857)	-5.33	V1500
V4642 Sgr	2000.1	S(60)	10.40 ± 0.40	Fe II	1530	...	bulge	8067 (7324 – 8810)
V4643 Sgr	2001.1	S(6)	7.70 ± 0.10	...	4700	...	DISC	5867 (4629 – 7965)	-10.70	...
V4739 Sgr	2001.7	S(3)	7.20 ± 0.10	He/N	5510	...	bulge	8002 (7267 – 8751)	-8.74	...
V4740 Sgr	2001.7	S(33)	6.70 ± 0.10	Fe II	BULGE	8033 (7288 – 8768)	-8.91	...
V4741 Sgr	2002.3	S(13)	9.20 ± 0.40	Fe II	2800	...	bulge	8066 (7312 – 8795)	-8.46	...
V4742 Sgr	2002.7	S(23)	7.90 ± 0.10	Fe II	2500	0.13362	DISC	3593 (2832 – 6016)	...	Ecl
V4743 Sgr	2002.7	S(12)	5.50 ± 0.20	Fe II, Ne	2400	0.2799	DISC	3717 (3253 – 4913)	-8.13	IP
V4744 Sgr	2002.8	...	$<9.7 \pm 0.20$	Fe II	1600	...	DISC	813 (633 – 1609)
V4745 Sgr	2003.3	J(190)	7.30 ± 0.10	Fe II	1350	0.20782	BULGE	8091 (7362 – 8834)	-7.86	IP?
V5113 Sgr	2003.7	J(48)	9.00 ± 0.30	Fe II	550	0.15002	bulge	8200 (7462 – 8932)	-6.19	...
V5114 Sgr	2004.2	S(21)	8.10 ± 0.10	Fe II	2000	...	bulge	7959 (7209 – 8702)	-8.26	...
V5115 Sgr	2005.2	S(13)	7.90 ± 0.10	He/N	1300	...	bulge	7749 (7014 – 8490)	-8.10	...
V5116 Sgr	2005.5	S(26)	7.60 ± 0.10	Fe II	970	0.12374	bulge	7573 (6837 – 8325)	-7.51	Ecl
V5117 Sgr	2006.1	S(23)	7.40 ± 0.30	Fe II	1600	...	disc?	2350 (1856 – 3745)	-5.70	...
V5558 Sgr	2007.3	J(157)	6.50 ± 0.10	Hybrid	1000	0.18581	DISC	2151 (2046 – 2319)	-7.64	...
V5579 Sgr	2008.3	D(13)	6.70 ± 0.10	Fe II	1500	...	BULGE	7945 (7210 – 8694)	-10.03	...
V5580 Sgr	2008.9	...	$<7.8 \pm 0.20$...	2500	34	BULGE	8143 (7420 – 8887)	...	RG
V5581 Sgr	2009.3	...	11.70 ± 0.20	Fe II	2600	1660	BULGE	8147 (7418 – 8886)	...	RG
V5582 Sgr	2009.1	J(90)	10.90 ± 0.30	He/N	...	0.15660	BULGE	8227 (7497 – 8963)	-5.75	...
V5583 Sgr	2009.6	S(7)	7.00 ± 0.20	He/N	2300	...	DISC	2383 (2142 – 3066)	-5.94	...
V5584 Sgr	2009.8	...	9.50 ± 0.20	Fe II	600	...	BULGE	8090 (7391 – 8821)	-7.83	...
V5585 Sgr	2010.1	O(25)	9.00 ± 0.20	Fe II	...	0.13753	BULGE	8312 (7613 – 9029)	-7.12	Ecl
V5586 Sgr	2010.4	...	11.10 ± 0.20	DISC	5195 (3856 – 7748)
V5587 Sgr	2011.2	C	11.20 ± 0.40	...	1300	...	bulge	8152 (7414 – 8890)	-6.46	PreERise
V5588 Sgr	2011.3	O(77)	11.30 ± 0.20	Hybrid	900	0.21432	bulge	7784 (7052 – 8529)	-7.34	...
V5589 Sgr	2012.4	S(13)	8.80 ± 0.10	Hybrid	5700	1.5923	bulge	7819 (7078 – 8550)	-7.68	SubG, Ecl
V5591 Sgr	2012.6	S(8)	9.60 ± 0.20	He/N	4200	...	bulge	7969 (7225 – 8716)	-9.37	...
V5592 Sgr	2012.6	D(28)	7.90 ± 0.30	Fe II	1700	...	BULGE	8192 (7500 – 8919)	-8.09	...
V5593 Sgr	2012.6	J(82)	11.00 ± 0.10	Fe II	940	...	BULGE	8092 (7358 – 8830)	-8.59	...
V5627 Sgr	1991	...	$<15.1 \pm 0.20$	0.11716	disc?	2829 (2783 – 8097)
V5666 Sgr	2014.2	J(201)	9.90 ± 0.10	BULGE	8010 (7315 – 8730)	-6.57	...
V5667 Sgr	2015.2	J(106)	9.10 ± 0.10	Fe II	300	...	BULGE	7694 (7009 – 8411)	-7.25	...
V5668 Sgr	2015.3	D(78)	4.30 ± 0.10	Fe II	2800	...	DISC	1290 (1045 – 1875)	-6.56	...
V5669 Sgr	2015.8	S	9.00 ± 0.10	Fe II	2000	...	BULGE	8304 (7603 – 9037)	-7.46	...
V5850 Sgr	2015.9	...	$<11.3 \pm 0.20$	bulge	8097 (7357 – 8838)
V5853 Sgr	2016.7	S(63)	11.50 ± 0.10	Fe II	bulge	8016 (7276 – 8761)	-8.91	...
V5854 Sgr	2016.6	...	$<11.1 \pm 0.20$...	2100	...	bulge	8087 (7349 – 8838)
V5855 Sgr	2016.9	J(19)	7.80 ± 0.10	Fe II	bulge	8049 (7312 – 8794)	-8.28	...
V5856 Sgr	2016.9	P(14)	5.90 ± 0.10	Fe II	DISC	3179 (2327 – 6029)	...	γ , V1500
V5857 Sgr	2018.4	...	$<10.6 \pm 0.20$	Fe II	387	...	bulge	8099 (7355 – 8844)
V5914 Sgr	2006.1	C	$<13.2 \pm 0.20$	0.82184	bulge	8144 (7396 – 8883)	...	SubG
V5926 Sgr	2013.3	S	$<16.4 \pm 0.20$	bulge	8131 (7390 – 8877)
V5980 Sgr	2010.1	...	$<12.1 \pm 0.20$	BULGE	8119 (7386 – 8875)
V6345 Sgr	2010.3	...	$<11.0 \pm 0.20$	Fe II	bulge	8147 (7396 – 8883)
V6566 Sgr	2020.2	...	$<11.1 \pm 0.20$	Fe II	1500	...	BULGE	8156 (7428 – 8892)
V6567 Sgr	2020.5	J	12.50 ± 0.10	Fe II	BULGE	8166 (7433 – 8905)	-6.56	...
V6568 Sgr	2020.6	...	$<9.9 \pm 0.20$	Fe II	4500	...	bulge	8150 (7392 – 8874)
V6593 Sgr	2020.8	...	$<11.1 \pm 0.20$	Fe II	bulge	8098 (7363 – 8841)
V6594 Sgr	2021.3	D(38)	9.50 ± 0.10	Fe II	1370	...	BULGE	8231 (7499 – 8963)	-6.01	...
V6595 Sgr	2021.3	S(15)	7.50 ± 0.10	Fe II, Ne	BULGE	7991 (7250 – 8736)	-9.03	...
T Sco	1860.4	S(18)	6.80 ± 0.40	GlobC	8845 (8317 – 9453)	-8.71	in M80
U Sco	RN	PP(3)	7.50 ± 0.10	He/N, Ne	5700	1.23055	DISC	6258 (5421 – 7428)	-7.10	SubG, Ecl, ΔP , \dot{P}
KP Sco	1928.5	...	8.59 ± 0.43	bulge	8085 (7344 – 8826)
V696 Sco	1944.3	...	$<7.1 \pm 0.25$	DISC	2322 (2119 – 2781)

Table 6 – *continued* Distances and Properties of All 402 Known Galactic Novae

Nova	Year	LC(t_3)	V_{peak}	Spec.	FWHM	P	Pop.	D (68% range)	M_V	Properties ^a
V697 Sco	1941.2	...	$<9.8 \pm 0.25$...	1550	1.26716	DISC	870 (780 – 1257)	...	SubG, Ecl
V707 Sco	1922.5	...	9.14 ± 0.45	bulge	8119 (7377 – 8855)	-7.42	...
V711 Sco	1906.3	S	9.08 ± 0.18	bulge	8128 (7400 – 8875)	-7.05	...
V719 Sco	1950.5	...	8.55 ± 0.32	Fe II	1800	0.43639	bulge	8057 (7315 – 8801)
V720 Sco	1950.6	...	$<6.9 \pm 0.25$	Fe II	1800	...	BULGE	7997 (7256 – 8743)
V721 Sco	1950.7	...	$<9.2 \pm 0.29$	DISC	1857 (1748 – 2028)
V722 Sco	1952.2	...	$<8.7 \pm 0.29$	bulge	8063 (7331 – 8812)
V723 Sco	1952.6	S(23)	8.09 ± 0.43	7.2	bulge	8070 (7319 – 8805)	...	SubG
V728 Sco	1862.8	...	$<5 \pm 0.20$	0.13834	DISC	1030 (930 – 1309)	...	Ecl
V745 Sco	RN	P(9)	9.40 ± 0.10	He/N	3600	2440	BULGE	8016 (7431 – 8640)	-8.22	RG, γ
V825 Sco	1964.4	...	$<10.9 \pm 0.36$	Ne	...	0.19166	BULGE	8184 (7456 – 8933)	...	Ecl
V902 Sco	1949.4	...	$<9.8 \pm 0.36$	BULGE	8096 (7363 – 8840)
V960 Sco	1985.7	...	$<10.5 \pm 0.20$	Fe II	BULGE	8193 (7454 – 8920)
V977 Sco	1989.6	...	$<10.4 \pm 0.20$	Fe II, Ne	...	26.2	DISC	467 (428 – 550)	...	RG
V992 Sco	1992.4	D(120)	7.70 ± 0.10	Fe II	800	0.1536	DISC	1815 (1622 – 2392)
V1141 Sco	1997.4	S(9)	8.50 ± 0.50	Fe II	3200	...	bulge	8096 (7358 – 8838)	-7.75	...
V1142 Sco	1998.8	S(22)	6.90 ± 0.40	...	3800	...	bulge	7985 (7257 – 8745)	-9.32	...
V1178 Sco	2001.4	...	10.20 ± 0.20	Fe II	1300	...	BULGE	8162 (7428 – 8900)	-6.75	...
V1186 Sco	2004.5	J(62)	9.70 ± 0.10	Fe II	500	0.20297	DISC	4099 (2634 – 7425)	...	Ecl
V1187 Sco	2004.6	S(17)	9.80 ± 0.10	Fe II, Ne	3000	...	DISC	4625 (3772 – 7155)
V1188 Sco	2005.6	S(23)	8.90 ± 0.10	Fe II	1730	...	bulge	8049 (7301 – 8787)	-8.82	...
V1280 Sco	2007.1	D(14)	3.78 ± 0.10	Fe II	1200	...	DISC	3502 (3309 – 3772)	-9.93	V1500
V1281 Sco	2007.1	S(26)	9.00 ± 0.30	Fe II	640	...	BULGE	8210 (7511 – 8935)
V1310 Sco	2010.2	J(113)	10.50 ± 0.30	Fe II	670	...	bulge	8027 (7292 – 8782)
V1311 Sco	2010.4	S(8)	8.60 ± 0.30	He/N?	3600	...	bulge?	8028 (7283 – 8768)	-8.87	...
V1312 Sco	2011.5	S(15)	9.50 ± 0.50	Fe II	1800	...	bulge?	8070 (7344 – 8827)
V1313 Sco	2011.8	S(18)	10.40 ± 0.50	Fe II	3000	50	BULGE	8272 (7561 – 8982)	...	RG
V1324 Sco	2012.5	D(30)	10.00 ± 0.10	Fe II	2000	...	bulge	7866 (7149 – 8617)	-8.07	γ , PreERise
V1533 Sco	2013.5	...	$<11.3 \pm 0.20$	bulge	8106 (7368 – 8852)
V1534 Sco	2014.2	S(9)	11.55 ± 0.20	He/N	7000	520	BULGE	8231 (7531 – 8936)	-6.47	RG
V1535 Sco	2015.2	P(20)	9.50 ± 0.20	He/N	2000	50	BULGE	7790 (7095 – 8540)	-7.44	RG
V1655 Sco	2016.5	D(50)	12.10 ± 0.10	Fe II	1400	...	bulge	8215 (7468 – 8938)	-6.01	γ
V1656 Sco	2016.8	...	11.43 ± 0.30	Fe II	1800	...	bulge	8073 (7335 – 8816)	-8.07	...
V1657 Sco	2017.2	...	$<12.7 \pm 0.20$	Fe II	2000	650	BULGE	8316 (7624 – 9047)	...	RG
V1658 Sco	2015.2	...	$<12.7 \pm 0.20$	Fe II	1810	...	BULGE	8141 (7406 – 8879)
V1659 Sco	2016.8	...	$<12.3 \pm 0.20$	Fe II	bulge	8135 (7396 – 8883)
V1660 Sco	2017.9	...	$<14.1 \pm 0.20$	He/N	BULGE	8140 (7399 – 8885)
V1661 Sco	2018.1	...	$<10.7 \pm 0.20$	Fe II	1950	...	bulge	8152 (7395 – 8880)
V1662 Sco	2018.2	...	$<10.5 \pm 0.20$	Fe II	1700	...	DISC	5370 (3853 – 8175)
V1663 Sco	2018.2	...	$<11.7 \pm 0.20$	Fe II	1900	...	bulge	8117 (7374 – 8861)
V1706 Sco	2019.5	J(170)	12.20 ± 0.40	Fe II	820	...	BULGE	8136 (7404 – 8878)	-7.31	...
V1707 Sco	2019.8	S(7)	11.80 ± 0.20	Fe II	6900	...	bulge	8038 (7297 – 8781)	-8.62	...
V1709 Sco	2020.3	D	13.60 ± 0.30	...	1300	...	BULGE	8067 (7335 – 8816)	-8.06	...
V1710 Sco	2021.4	S(11)	8.60 ± 0.10	Fe II	2380	...	disc?	5258 (3200 – 8228)
V1711 Sco	2021.6	C(38)	11.09 ± 0.10	Fe II	1800	...	bulge	8095 (7359 – 8838)	-7.67	...
Nova 1437 Sco	1437.2	...	$<3 \pm 0.20$	DISC	1030 (999 – 1073)
EU Sct	1949.6	S(42)	8.40 ± 0.10	Fe II	...	68	DISC	7823 (6853 – 9771)	-8.67	RG
FS Sct	1952.5	J	9.43 ± 0.36	Fe II	...	5.7	DISC	5176 (4072 – 8034)	...	SubG
FV Sct	1960.5	...	$<11.1 \pm 0.45$	disc	6351 (3699 – 9343)
V366 Sct	1961.4	...	$<11.3 \pm 3.01$	DISC	8466 (6289 – 13423)
V368 Sct	1970.6	P(30)	6.90 ± 0.50	Fe II	DISC	2452 (1950 – 4181)
V373 Sct	1975.5	J(79)	6.10 ± 0.10	0.81910	DISC	1458 (1229 – 2343)	-5.43	SubG
V443 Sct	1989.7	J(60)	8.50 ± 0.10	Fe II	1400	...	DISC	2802 (2193 – 4583)
V444 Sct	1991.7	P(23)	10.80 ± 0.40	Fe II, Ne	DISC	7381 (5600 – 10718)
V463 Sct	2000.2	J(24)	10.30 ± 0.40	Fe II	990	...	bulge	8076 (7334 – 8820)	-6.72	...
V476 Sct	2005.7	S(28)	11.09 ± 0.10	Fe II	1200	...	DISC	7820 (6247 – 10794)	-9.27	...
V477 Sct	2005.8	S(6)	9.80 ± 0.30	Fe II	2900	...	DISC	6258 (4426 – 9152)
V496 Sct	2009.8	S(98)	7.20 ± 0.20	Fe II	1200	...	DISC	4517 (3629 – 6664)	-7.84	...
V611 Sct	2016.8	...	$<13.4 \pm 0.20$	He/N	DISC	8090 (5758 – 12416)
V612 Sct	2017.6	J(236)	8.50 ± 0.10	Hybrid, Ne	1180	...	bulge	8063 (7330 – 8811)	-8.05	...
V613 Sct	2018.6	S(66)	10.70 ± 0.10	Fe II	1800	...	BULGE	8091 (7354 – 8835)	-7.87	...
V659 Sct	2019.9	...	8.36 ± 0.10	Hybrid	DISC	5539 (3639 – 8589)
X Ser	1903.2	S(730)	8.74 ± 0.23	1.478	DISC	3089 (2722 – 3843)	-4.48	SubG, DN

Table 6 – *continued* Distances and Properties of All 402 Known Galactic Novae

Nova	Year	LC(t_3)	V_{peak}	Spec.	FWHM	P	Pop.	D (68% range)	M_V	Properties ^a
CT Ser	1948.3	...	$<7.7 \pm 0.23$	He/N	...	0.195	DISC	2551 (2330 – 2904)
DZ Ser	1960.6	...	$<13.1 \pm 0.36$	He/N	BULGE	8142 (7396 – 8883)
FH Ser	1970.1	D(62)	4.50 ± 0.10	Fe II	DISC	1024 (970 – 1103)	-7.41	Shell
LW Ser	1978.2	D(52)	8.30 ± 0.10	Fe II	bulge	7661 (6933 – 8412)	-7.33	...
MU Ser	1983.1	...	7.70 ± 0.40	He/N	1230	...	BULGE	7262 (6503 – 8025)	-7.85	...
V378 Ser	2005.2	J(93)	11.60 ± 0.40	Fe II	1100	...	BULGE	8238 (7500 – 8969)	-5.27	...
V556 Ser	2014.0	...	$<12.3 \pm 0.20$	Fe II	1145	...	BULGE	8166 (7420 – 8903)
V670 Ser	2020.2	S(6)	12.50 ± 0.40	Fe II	4200	...	bulge?	8083 (7345 – 8826)	-7.93	...
XX Tau	1927.9	D(43)	5.59 ± 0.25	Fe II	...	0.12936	DISC	2041 (1711 – 2904)	-6.89	NonOrbP
NR TrA	2008.2	J(61)	8.60 ± 0.20	Fe II	...	0.2192	DISC	4864 (4212 – 6254)	-5.52	Ecl
RW UMi	1956.7	...	$<5.9 \pm 0.21$	0.05912	DISC	1993 (1721 – 2592)	...	<Gap, V1500
CN Vel	1905.9	S	$<9.9 \pm 0.23$	0.2202	DISC	4227 (3654 – 6186)
CQ Vel	1940.3	S(50)	8.30 ± 0.23	0.11272	DISC	3061 (2372 – 5486)	-5.96	...
V382 Vel	1999.4	S(13)	2.80 ± 0.10	He/N, Ne	2400	0.1461	DISC	1531 (1454 – 1638)	-8.50	...
V549 Vel	2017.8	J(118)	9.10 ± 0.30	Fe II	...	0.40317	DISC	2056 (1753 – 5052)	...	γ
LU Vul	1968.8	S(21)	8.19 ± 0.45	He/N	820	...	DISC	4998 (3952 – 8687)
LV Vul	1968.3	S(38)	4.50 ± 0.10	Fe II	DISC	2887 (2420 – 4234)	-9.57	Shell
NQ Vul	1976.8	D(50)	6.20 ± 0.10	Fe II	...	0.14626	DISC	1210 (1128 – 1350)	-7.07	Shell
PW Vul	1984.6	J(116)	6.40 ± 0.10	Fe II	...	0.12858	DISC	2114 (1901 – 2603)	-6.93	NonOrbP, Shell
QU Vul	1985.0	P(36)	5.30 ± 0.10	Fe II, Ne	...	0.11176	DISC	1742 (1432 – 2772)	-7.61	Ecl, Shell
QV Vul	1987.9	D(47)	7.10 ± 0.10	Fe II	920	...	DISC	2808 (2348 – 4011)	-6.38	Shell
V458 Vul	2007.6	J(20)	8.10 ± 0.20	Hybrid	1750	0.06812	DISC	5204 (4357 – 7750)	-7.03	<Gap, InPNeb
V459 Vul	2008.0	S(30)	7.60 ± 0.10	Fe II	910	...	DISC	3971 (3226 – 5608)	-8.06	...
V569 Vul	2019.7	...	$<16.3 \pm 0.20$...	1800	...	DISC	7839 (5436 – 13726)
V606 Vul	2021.6	D(96)	10.10 ± 0.10	Hybrid	1700	...	DISC	4827 (3578 – 7811)

^a Novae below and inside the nova Period Gap from 0.071–0.111 days are denoted with **<Gap** and **inGap**. Novae with subgiant companion stars (roughly $0.6 < P < 10$ days) and red giant companion stars (roughly $P > 10$ days) are marked as **SubG** and **RG**. Novae whose light curves display eclipses are denoted with **Ecl**, display dwarf nova eruptions with **DN**, display inexplicable pre-eruption rises with **PreERise**, display post-eruption dips with **PostEDip**, display coherent and stable periods that are certainly not orbital or rotational with **NonOrbP**, display very large amplitude irregular variability in quiescence with **LargeAmpVar**, and display various types of inexplicable rebrightenings are notated with **Rebrighten**. **V1500** indicates the mysterious V1500 Cyg stars where the post-eruption brightness many decades after the end of the eruption remains at least $10\times$ brighter than the pre-eruption level. **InPNeb**; V458 Vul is the only nova to be at the centre of an observed ordinary planetary nebula. Novae visible with γ -ray emission by the *Fermi* spacecraft are marked γ . Novae for which I have measured the steady period change between eruptions are marked with \dot{P} , while those for which I have measured the change in the orbital period sharply across a nova eruption are marked with ΔP . V1500 Cyg is the only nova known to be an asynchronous polar (**AP**). Novae inside host globular clusters are listed with **in M14** or **in M80**. Binaries that are either confidently or likely Intermediate Polars (**IP** or **IP?**) are identified as in the catalogue of K. Mukai (<https://asd.gsfc.nasa.gov/Koji.Mukai/iphome/catalog/alpha.html>). Startlingly, V2487 Oph suffers the most-energetic and the most-frequent **Superflares** out of the many classes of stars that display bright optical flares caused by stellar magnetic reconnection.

$E(B - V)$ and its one sigma error bars, in units of magnitudes, for all 402 novae. Many of these are taken from Özdönmez et al. (2018), or from subsequent literature, or from my own light curve analyses, or from prudent estimates based on the upper limits from Schlafly & Finkbeiner (2011). The next column gives the t_2 value, which is the number of days over which the nova light curve declines from its highest peak until the last time the nova fades by more than 2.0 mags from the peak. The last extra column gives the *Gaia* DR3 parallax and its one sigma uncertainty, as in Table 5.

Table 6 is intended to be an exhaustive summary of all the known properties of all 402 known galactic novae. The one line of information gives a comprehensive summary of all its known properties, and each line reveals the ‘personality’ of each nova. This full table can be used for looking up properties of individual novae, for standardizing the prior results from the long history of measuring novae, and for demographic studies of a wide variety of nova properties.

7 APPLICATIONS

7.1 Nova Disc Scale Height

Duerbeck (1984) collects nine measures of the exponential scale height for novae, with values ranging from 72–440 pc, and then went on to use 20 novae to derive his own scale height of 125 pc. The height of each nova above the central plane of our galaxy, Z , is $D \sin(b)$. My histograms of the distances from the galactic plane, $|Z|$, shows that all sets of disc novae have a sharp drop in numbers from $|Z|=0$, and the distributions are close to exponential. The distribution can be accurately represented by the exponential scale height, which is the same as the average, $\langle |Z| \rangle$.

The derived $\langle |Z| \rangle$ will vary with the selection of disc novae included in the average. If the set for averaging includes novae with large uncertainty in D , then $\langle |Z| \rangle$ will systematically grow in size to be comparable to the error bars. So the set of novae for averaging should be restricted to only the best-measured novae with uncertainties substantially smaller than 150 pc or so. But if we make the set too small, then the scale height will be uncertain due to small-number statistics. Further, some sort of volume-limited sample is needed to minimize selection effects. To avoid edge effects in this volume, we

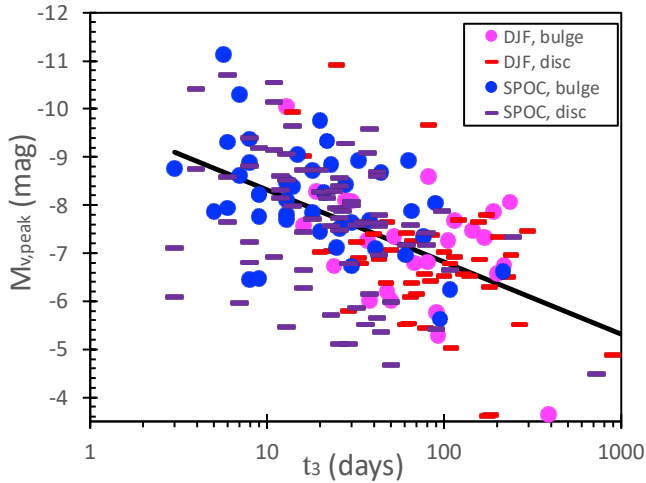


Figure 4. Absolute magnitude at peak ($M_{V,peak}$) versus decline rate (t_3). This plot shows the MMRD for 192 novae with measured t_3 and the uncertainty in $M_{V,peak}$ of less than 1.0 mag. We see a significant correlation, $M_{V,peak} = -7.6 + 1.5 \log(t_3/30)$, as marked by the slanted line. But we also see a huge scatter, such that the ‘correlation’ just looks like a round blob. The only reason that the correlation is significant is because I have 192 novae. All the prior samples testing the MMRD have had much fewer novae, and thus the many samples have not shown any significant MMRD relation, while one prior sample has randomly happened to show a poor MMRD. The MMRD shown here supersedes all prior galactic results. The conclusion is that the MMRD does really exist, but the huge scatter dominates over the effect and thus the relation is not useable for any purpose that I can think of.

need to use an infinite cylinder, centred on the Sun, perpendicular to the galactic plane. Further, I have not used any novae with $\theta_{GC} < 20^\circ$, so as to avoid any possible confusion with bulge novae.

I have adopted a middle set, with a cylinder radius of 2000 pc and requiring that the uncertainty in Z be less than 30 pc. This results in a set of 34 disc novae with good distances. This set has $\langle |Z| \rangle = 140$ pc. The uncertainty is defined by the reasonable variations for inclusion in the averaging set, with this being ± 10 pc. So I conclude that the novae are distributed exponentially above and below the galactic plane, with an exponential scale height of 140 ± 10 pc. This $\langle |Z| \rangle = 140$ pc value is used in equation (6) to calculate the final nova distances, as in Section 6 and Table 6.

7.2 Absolute Magnitude At Peak Light In The V-band

What is the average $M_{V,peak}$? Schaefer (2018) used *Gaia* DR2 data for novae with accurate parallaxes to yield an average of -7.0 with an RMS scatter of 1.4 mag. Now, with the 213 novae in Table 6, the average is -7.45 mag with an RMS scatter of 1.33 mag. Various subsets give similar values, with a variation over 0.2 mag or so, for example, the 15 novae with error bars < 0.30 mag have an average of -7.51 mag with an RMS scatter of 1.35 mag. For the full set of 213 novae, the top end of the luminosity distribution has 8 novae evenly spread over the range $-10.0 > M_{V,peak} > -11.13$. These include the famous V1500 Cyg at -10.38 , and the extreme case is the bulge nova V3661 Oph at -11.13 . At the low-luminosity end, 6 novae span $-3.62 > M_{V,peak} > -5.0$. The extreme case is V972 Oph at -3.62 mag. Three of the six cases have flat-topped F-class light curves (DO Aql, V1310 Sgr, and BT Mon), pointing to this class being systematically low-energy eruptions. For all of these extreme cases, I see no indications that the $M_{V,peak}$ values have any large

measurement or systematic errors past what is expressed in the stated error bars. So it appears that the range of the nova phenomenon extends from at least -5.0 to -10.0 .

These D and $M_{V,peak}$ values were derived with an assumed prior for peaks of -7.0 ± 1.4 mag. Should this be updated to the new average of -7.45 ± 1.33 mag? Or should we change the P_{peak} priors to represent the various correlations with light curve and spectral classes (see below)? The answer is clearly ‘no’, for two strong reasons. First, the Bayesian method requires the use of *prior* information, so it is incorrect to feed the calculated results back into the calculation. Second, doing so would make for little difference anyway. That is, the adopted error bar of ± 1.4 mag is already so weak that any change to the adopted $M_{V,peak}$ will lead to changes in D that are greatly smaller than the quoted error bars.

Now with 213 good measures, I can search for correlations between $M_{V,peak}$ and any of many other properties listed in Table 6. Most properties have no significant correlation with the peak luminosity, including the various spectral classes (e.g., Fe II, He/N, and Neon), the shell expansion velocity (as measured by the FWHM of the Balmer lines), the status as a RN, and the galactic population (disc or bulge). I find only two properties with significant correlations.

The first correlation is with the light curve classification. The S-class, P-class, O-class, and C-class novae are for the high-energy novae (i.e., with large FWHM, He/N spectral class, high white dwarf masses, and fast declines), and these are grouped together here. The D-, J-, and F-classes are for low-energy novae, and are grouped together here. With 124 SPOC novae, the average is -7.75 ± 0.12 . With 75 DJF novae, the average is -6.95 ± 0.15 . So just by looking at the shape of the light curve, we can identify whether the nova peaks at relatively high-or-low luminosity.

The second correlation is that $M_{V,peak}$ is a function of the decline rate of the light curve (expressed as t_3 or t_2). Specifically, the 92 fast novae (say, with $t_3 < 30$ days) have $\langle M_{V,peak} \rangle$ equal to -8.13 ± 0.13 , while the 20 slow novae (with $t_3 > 100$ days) have -6.80 ± 0.25 . That is a 1.33 mag difference, which is a factor of $3.4 \times$ in peak luminosity. Fig. 4 shows a plot of $M_{V,peak}$ versus t_3 , and we see a significant trend, despite the huge scatter making the data points looking like a round blob. The same trend with the same large scatter is seen when only using novae with the uncertainty in $M_{V,peak}$ that is < 0.5 mag. This trend is identical for SPOC versus DJF light curve classes, and identical for bulge versus disc novae. A least square fit gives the relation $M_{V,peak} = -7.6 + 1.5 \log(t_3/30)$, for t_3 in units of days. The existence of this correlation is significant at the 8.6-sigma level. But the scatter about this relation is huge, so the correlation is significant only because I am using 192 novae. The scatter has an RMS of 1.0 mag on top of the measurement errors. The relevant figure is that the disagreement from model to observation has the 68 per cent range of 2.4 mag and the total range of 6.2 mag. That is, the 1-sigma uncertainty in using this relation results in a range of luminosity by a factor of $10 \times$. With the very large scatter around the relation, there is little utility for physical models of any specific system. With this large scatter, the use of this relation is a negligible improvement over using a simple average of -7.0 ± 1.4 mag.

This relation fits into a long history of the so-called ‘Maximum Magnitude versus Rate of Decline’ (MMRD). The MMRD was first put forth for novae in the Andromeda Galaxy (Hubble 1929), with follow-ups, extensions, and refinements by many workers from the 1950s until recently, with the first theoretical explanation by Shara (1981). MMRD relations have been presented with many formulations, involving magnitudes at various times in the eruption, involving B- and V-magnitudes, involving decline rates over 2 and 3 magnitudes, and involving logarithms, broken logs, and arc-tangents. The

best expression of the MMRD was in Downes & Duerbeck (2000), with no improvements since then. Historically, the MMRD has been heavily used, largely because it was the only way to estimate distances to most novae. The MMRD has always been known to be poor, due to the huge scatter in the relation. Starting with Kasliwal et al. (2011), the relation fell into disrepute when the novae in the galaxies M31, M81, M82, NGC 2403, and NGC 891 did *not* display anything like the MMRD. They also showed that the RNe do not obey the MMRD, nor do the latest theory models of Yaron et al. (2005). Then Shara et al. (2017b) showed that the novae in M87 do *not* follow the MMRD. Then Schaefer (2018) used *Gaia* DR2 parallaxes to show that 26 galactic novae in the ‘Gold’ sample followed a shifted MMRD with huge scatter, while the 13 and 23 galactic novae in the ‘Silver’ and ‘Bronze’ samples do not show anything like any MMRD. The Gold sample is largely the same as the Downes & Duerbeck sample, so we only really have just one sample of novae that poorly follows the MMRD. In stark opposition, we have the MMRD being denied for two other galactic samples, the RNe, theory models, and by novae in six external galaxies.

Now, with 192 novae and the best distances, my confirmation of the MMRD supersedes all the prior results for our Milky Way. Presumably the old samples either showed or denied the poor MMRD due to the randomness of small samples out of a highly scattered distribution. That is, the Downes & Duerbeck sample displayed a poor MMRD by the random happenstance of the novae going into their sample, while other samples had the happenstance to have the scatter being too large to allow the MMRD to be visible. The point is that the MMRD is now seen to be real, even though the scatter is so large as to debilitate the use of this relation. We are now left with the question as to why the Milky Way has a poor MMRD, while the six external galaxies do not show it at all. I think that the reconciliation is that the searches in each external galaxy produces a relatively small number of novae, and the small numbers with huge scatter will always make for no significant detection of the MMRD. That is, the huge scatter means that the MMRD can only be confidently detected when a large number of novae are included (like 192 galactic novae in this paper), whereas no MMRD can be significant when relatively small numbers of novae are included.

In the end, we are left with $\langle M_{V,peak} \rangle = -7.45 \pm 1.33$ mag being nearly as good a description of the data as $M_{V,peak} = -7.6 + 1.5 \log(t_3/30)$. The MMRD is definitely a real effect for galactic novae, and likely for external galaxies, despite the large scatter. The theory explanation is as given by Shara (1981), with both $M_{V,peak}$ and t_3 directly tied to the white dwarf mass. Despite now having a significant existence, the MMRD has so much scatter that it is useless for evaluating the distance to any particular novae.

7.3 Bulge Versus Disc Novae

Now, I have a confident list of all known bulge novae and disc novae, plus an exhaustive list of their primary known properties. So I can systematically make a comprehensive study of the two populations.

For this, I have used the 161 novae identified as ‘BULGE’ or ‘bulge’ and the 224 novae identified as ‘DISC’. The results are in Table 7. Each line presents a property for which either a fraction or an average can be derived. The parenthetical numbers are either the numbers of novae in the fraction, or the number of novae in the average along with the overall RMS of the population. The population differences in $\langle M_V \rangle$, the median FWHM of the velocity width of the Balmer lines, and the median t_3 decline speed are all within one-sigma. Similarly, the fraction of novae that are SPOC (i.e., with light curve classes S, P, O, or C), as well as the fractions for the various

Table 7. Comparing Bulge and Disc Populations

Property	Bulge Novae	Disc Novae
$\langle M_V \rangle$ (mag)	-7.73 (26, ± 1.28)	-7.51 (45, ± 1.32)
Median FWHM (km/s)	1500 (93, ± 1700)	1670 (116, ± 1220)
Median t_3 (days)	28 (79, ± 67)	38 (163, ± 110)
SPOC fraction	0.62 (51 / 82)	0.61 (105 / 173)
Fe II fraction	0.80 (77 / 96)	0.72 (106 / 147)
He/N fraction	0.14 (13 / 96)	0.18 (27 / 147)
Hybrid fraction	0.06 (6 / 96)	0.09 (13 / 147)
Neon fraction	0.08 (8 / 100)	0.19 (29 / 151)
Helium fraction	0.00 (0 / 100)	0.01 (1 / 151)
Subgiant fraction	0.22 (8 / 37)	0.18 (21 / 115)
Red giant fraction	0.35 (13 / 37)	0.05 (6 / 115)

spectral classes, are indistinguishable between bulge and disc novae. Further, the fraction of novae with subgiant companion stars (i.e., those with $0.6 < P < 10$ days) is the same between the populations.

I can find only one property for which the bulge and disc novae differ, and that is the red giant fraction. The nova systems with red giant companions are easily recognized, even out past D_{GC} , by their infrared flux whose spectral energy distribution is a warm blackbody, shining above the usual blue accretion disc flux (Schaefer 2022). Their orbital periods are from 10 days out to near 2440 days. The bulge novae have a red giant fraction of 35 ± 8 per cent, while the disc novae have a red giant fraction of 5 ± 2 per cent. This is a highly significant difference. A similar result was found by Schaefer (2022).

So the only difference between the bulge and disc populations is that the bulge has a high red giant fraction. The first-glance explanation is that the bulge novae are older, on average, than disc novae, so the nascent wide binaries formed with a white dwarf will have longer time for the companion to evolve to its red giant stage and come into contact. But my simplistic modeling suggests that this explanation cannot be fine tuned to get such a large difference. Further, such an explanation has a hard time allowing for the subgiant fractions to be equal between the two populations. Another mystery arises because the novae with red giant companions in the Andromeda Galaxy are consistent with being entirely in the *disc* population (Williams et al. 2016). I am not aware of any selection effect or systematic problem that can account for the large differences in the red giant fractions. So I am left with no useable explanation for the Milky Way novae having the systems with red giants concentrated in the bulge population.

The bulge novae are neither faster or slower, neither brighter or dimmer than disc novae, nor are the bulge novae different in light curve or spectral class. Other than the red giant fraction, the bulge novae are indistinguishable from the disc novae.

7.4 RS Oph Is Powered By Roche Lobe Overflow

The issue of the distance to RS Oph determines the nature of the accretion in the binary (Schaefer 2009; Wynn 2008). For distances < 2000 pc, the companion must be substantially smaller than its Roche lobe, so the accretion can only come by the white dwarf capturing some fraction of the red giant’s stellar wind. For distances over ≥ 2700 pc, the companion must be so large as to fill its Roche lobe, and the accretion would be entirely by Roche lobe overflow.

Historically, the first widely seen distance estimates were those of Hjellming et al. (1986) and Cassatella et al. (1985), with extinction distances of 1600 pc. Most later papers explicitly cited these papers, and 1600 pc became the default by repetition. Then modelers took results assumed from this distance (the system having wind accretion)

to calculate models, and then derived distances comparable to 1600 pc, a circular conclusion. In an uncritical review of RS Oph distances up until 2006, Barry et al. (2008) merely collected the many published distance measures and took the median, to get 1400 pc. The legacy of this band-wagon-effect (Schaefer 2008) has continued to the current time, with the most recent RS Oph publication (Cheung et al. 2022) adopting 1600 pc as explicitly attributed to the Hjellming paper.

The problems for this vote-on-the-distance result are that the distances reported by both Hjellming⁵ and Cassatella⁶ are certainly and greatly mistaken. Further errors in the old distance estimates to RS Oph are listed in Schaefer (2009), while the real uncertainties in many of the old papers are greatly larger than reported (Schaefer 2009; 2018) so that the results are too poor to be useful. Further, with the observed red giant wind velocities, the fraction of the stellar wind captured by the white dwarf must be greatly too small to allow for RN eruptions every 9–27 years (Schaefer 2009).

Into this poor history, we now have a good parallax from *Gaia* DR3 of 0.373 ± 0.023 mas. With a fractional error this small, the simple calculation returns a good distance, which is 2680 ± 165 pc. With the Bayesian calculation and the priors, RS Oph has a best-estimate distance of 2710 pc, with the central 68 per cent range 2575–2908 pc. Now, *Gaia* has returned a decisive answer, with RS Oph near 2710 pc, and the companion star is the same size as its Roche lobe, so the accretion in the system is entirely by Roche lobe overflow.

8 ACKNOWLEDGEMENTS

In this massive data mining program, the real heroes are the many thousands of observers contributing their observations, plus the hundreds of workers supporting and archiving the analysis and data. Of particular importance are the builders, operators, analysts, and archivists of the *Gaia* mission. (This work has made use of data from the European Space Agency (ESA) mission *Gaia* (<https://www.cosmos.esa.int/gaia>), processed by the *Gaia* Data Processing and Analysis Consortium (DPAC, <https://www.cosmos.esa.int/web/gaia/dpac/consortium>).

9 DATA AVAILABILITY

The *Gaia* data are publicly available on-line. The nova light curve and eruption data are from the cited literature (and references therein), and the public databases of the AAVSO. The resultant measures and analysis are completely presented in the Tables.

⁵ The mistake in Hjellming et al. (1986) was to adopt a linear calibration for their measure of extinction, with this only being reasonable for a line of sight that keeps exactly in the galactic plane. RS Oph has a galactic latitude of $b=+10.37^\circ$, so the line of sight to RS Oph will be 300 pc out of the plane for a distance of 1600 pc and far outside almost all of the galaxy's extinction. That is, Hjellming's calibration relation is greatly wrong, and the distance estimate is greatly wrong. In reality, the observed extinction is close to the maximum extinction along the entire line of sight through our galaxy, and this demonstrates only that the RS Oph distance has a lower limit of something like 1000 pc, beyond which the line of sight has no significant galactic absorption.

⁶ Cassatella et al. (1986) noted that they could not find any absorption at a radial velocity corresponding to the Carina Arm of our Milky Way (at a distance of 2000 pc), and concluded that RS Oph must be closer than 2000 pc. The error of Cassatella is in not realizing that at 2000 pc and with $b=10.37^\circ$, the line of sight passes 370 pc above the galactic centre plane. With the line-of-sight passing far above all of the gas and dust in the Carina Arm, there is no limit on the distance from this basis.

REFERENCES

- Bailer-Jones, C. A. 2015, *PASP*, 127, 994
 Barry R. K. et al., 2008, in Evans A. et al., eds, *ASP Conf. Ser. Vol. 401, RS Ophiuchi (2006) and the Recurrent Nova Phenomenon*. Astron. Soc. Pac., San Francisco, p. 52
 Cassatella A., Hassall B. J. M., Harris A., Snijders M. A. J., 1985, ed. W. R. Burke, *ESA SP-236, Recent Results on Cataclysmic Variables*. European Space Agency, Noordwijk, p. 281
 Cheung C. C., et al. 2022, *ApJ*, in press, see arXiv:2207.02921
 Della Valle M., Livio M., 1994, *A&A*, 286, 786
 Downes R. A., Duerbeck H. W., 2000, *AJ*, 120, 2007
 Downes R. A., Webbink R. F., Shara M. M., Ritter H., Kolb U., Duerbeck H. W., 2001, *PASP*, 113, 764
 Duerbeck H. W. 1984, *ApSSS*, 99, 363
 Duerbeck H. W. 1987, *Space Sci Rev*, 45, 1
 Gaia Collaboration et al., 2016, *A&A*, 595, A1
 Gaia Collaboration et al., 2022, *A&A*, in preparation
 Hachisu I., Kato M., 2021, *ApJS*, 253, 27
 Harrison T. E., Bornak J., McArthur B. E., Benedict G. F., 2013, *ApJ*, 767, 7
 Hatano K., Branch D., Fisher A., Starrfield S., 1997, *MNRAS*, 290, 113
 Hjellming R. M., van Gorkom J. H., Seagquist E. R., Taylor A. R., Padin S., Davis R. J., Bode M. F. 1986, *ApJ*, 305, L71
 Hubble E., 1929, *ApJ*, 69, 103
 Jacoby G. H., et al. 1992, *PASP*, 104, 599
 Kasliwal, M. M., Cenko, S. B., Kulkarni, S. R., Ofek, E. O., Quimby, R., & Rau, A. 2011, *ApJ*, 735, 94
 Li L., et al., 2018, *ApJ*, 858, 75
 Luri, X., Brown, A. G. A., Sarro, L. M., Arenou, F. et al. 2018, *A&A*, 616, A9
 Malkin Z., 2012, arXiv:1202.6128
 Mróz P. et al., 2015, *ApJS*, 219, 26
 Özdoğan E., Ege E., Güver T., Ak T., 2018, *MNRAS*, 476, 4162
 Pagnotta A., Schaefer B. E., 2014, *ApJ*, 788, 164
 Patterson J. et al., 2022, *ApJ*, 924, 27
 Payne-Gaposchkin C. 1964, *The Galactic Novae*, Dover, New York
 Ramsay G., Schreiber M., Gänsicke B., Wheatley P., 2017, *A&A*, 604, A107
 Reid M. J., 1993, *ARAA*, 31, 345
 Salazar I., LeBleu A., Schaefer B., Landolt A., 2017, *MNRAS*, 469, 4116
 Schaefer B. E., 2008, *ApJ*, 697, 721
 Schaefer B. E., 2009, *AJ*, 135, 112
 Schaefer B. E., 2010, *ApJS*, 187, 275
 Schaefer B. E., 2018, *MNRAS*, 481, 3033
 Schaefer B. E., 2022, *MNRAS*, in press
 Schlafly E.F., Finkbeiner D.P., 2011, *ApJ* 737, 103
 Shafter A. W., 1997, *ApJ*, 487, 226
 Shafter A. W., 2008, in Bode M. F., Evans A., eds, *Classical Novae*, second edition. Cambridge University Press, Cambridge, p. 335
 Shara M. M., 1981, *ApJ*, 243, 926
 Shara M. M. et al., 2017a, *Nature*, 548, 558
 Shara M. M. et al., 2017b, *ApJ*, 839, 109
 Sokoloski J. L., Crotts A. P. S., Lawrence S., Uthas H., 2013, *ApJ*, 770, L33
 Strophe R. J., Schaefer B. E., Henden A. A., 2010, *AJ*, 140, 34
 van den Bergh S., Younger P. F. 1987, *A&ASuppl*, 70, 125
 Vasiliev E., Baumgardt H., 2021, *MNRAS*, 505, 5978
 Walter F. M., Battisti A., Towers S. E., Bond H. E., Stringfellow G. S., 2012, *PASP*, 124, 1057
 Warner B., 2008, in *Classical Novae*, M. F. Bode M. F., Evans A., eds, Cambridge Univ. Press, Cambridge
 Williams S., Darnley M., Bode M., Shafter A., 2016, *ApJ*, 817, 143
 Wynn G. A., 2008, in Evans A. et al., eds, *ASP Conf. Ser. Vol. 401, RS Ophiuchi (2006) and the Recurrent Nova Phenomenon*. Astron. Soc. Pac., San Francisco, p. 73
 Yaron, O., Prialnik, D., Shara, M. M., & Kovetz, A. 2005, *ApJ*, 623, 398

This paper has been typeset from a $\text{\TeX}/\text{\LaTeX}$ file prepared by the author.